Materials Today Advances 6 (2020) 100058

Contents lists available at ScienceDirect

Materials Today Advances

journal homepage: www.journals.elsevier.com/materials-today-advances/

Solid-state photoswitching molecules: structural design for isomerization in condensed phase

A. Gonzalez, E.S. Kengmana, M.V. Fonseca, G.G.D. Han*

Department of Chemistry, Brandeis University, 415 South Street, Waltham, MA, 02453, USA

ARTICLE INFO

Article history:
Received 13 November 2019
Received in revised form
3 February 2020
Accepted 5 February 2020
Available online 14 March 2020

Keywords:
Photoswitches
Thin films
Crystals
Covalent functionalizations

ABSTRACT

Photoswitching dynamics of common organic photoisomers in solid state are often reduced compared to the solution state due to the close packing of molecules that limits structural changes. The facile solid-state switching of photoisomers has implications in developing novel light-controlled devices such as actuator, field-effect transistor, and photodetector, as well as photon energy storage materials that can be charged by light and release thermal energy upon triggering. Thus, the solid-state photoswitching of organic molecules has been studied in relation to the structural characteristics, and various effective methods to enhance the switching in condensed phases have been developed. This review highlights isomerization dynamics of common photoswitches in solid and then introduces important strategies for facilitating the switching dynamics, including the covalent functionalization methods for small-molecule photoswitches as well as the incorporation of various templates such as porous medium, nanoparticle, and host-guest structure. Furthermore, the solid-state switching of molecules at the interface with inorganic substrates including 2D materials and the microscopy techniques for the characterization will be further described.

1. Introduction

Photoswitches are molecules that undergo structural changes in response to light irradiation. The molecules generally possess two stable isomeric forms that are under equilibrium and can be reversibly obtained by irradiation and thermal activation [1]. As a result of the isomerization and the distinct molecular properties of isomers, such as polarity [2], steric hindrance [3], and optical properties [4], the photoswitches have been incorporated to various platforms to exert light-induced changes to the bulk properties including surface energy [5], morphology [6], and color [7] of bulk solids. Accordingly, various applications of photoswitches have been developed, taking advantage of the fast, drastic, and reversible change in properties that can be addressed by light illumination. Examples include the light-induced actuation of thin films [8], photon energy storage in bulk materials [9,10], light-activated drug release from solid carriers [11], photomagnetic switching [12,13], and hydrophobicity switching of heterogeneous surface [14].

However, the photoswitching molecules incorporated to solid platforms often exhibit limited switching due to the severe steric hindrance induced by the close packing of molecules, particularly in crystalline lattice, which remains a challenge [15]. This incomplete switching or the lack of switching of molecules results in the absence of functionality that can be modulated by light irradiation. The photoisomerization behavior of switches is first studied in dilute solutions by UV–vis absorption or nuclear magnetic resonance spectroscopy, which reflects the maximum switchability or photostationary state of each isomer, due to the facile structural change in molecules in the solvated state. The dilute dispersion of molecules in amorphous [16] and elastomeric polymer matrix [17] also exhibits similar behavior to solution-state switches due to the unhindered environment for rotation or inversion of molecular structures.

The dilute solutions or dispersion systems, however, lower the density of photoactive units per volume or mass, leading to the insufficient change in bulk properties. In particular, the photon energy storage in solid-state photoswitching materials requires high gravimetric density of energy (J/g) for thermal applications [9], which indicates the importance of facile switching of photoactive moieties at high density. It is indeed a significant challenge to balance the molecular density with the free space between

* Corresponding author.
E-mail address: gracehan@brandeis.edu (G.G.D. Han).

https://doi.org/10.1016/j.mtadv.2020.100058

molecules in condensed phase. The strategies to tackle this challenge have been developed, particularly through chemical modification of pristine photoswitching units.

In this review, we will highlight the effective strategies applied to organic photoswitches that are either traditional or newly developed, to maximize the degree of isomerization in solid state. Different strategies are applied to photoswitches depending on the structure; thus, we first introduce the general photoswitching schematics for the switches discussed in this review. There is a plethora of molecules capable of photoinduced isomerization, each with their own unique structural changes (Scheme 1). Photoisomerization requires a change in volume, whether the mechanism be through rotation or inversion about the original double bond, through ring-opening, or a combination of the two.

1.1. Photoswitches that require large volume change

Photoswitches undergoing large structural changes include azobenzenes, hydrazones, and indigoids, all of which involve the isomerization about a double bond through *E*-to-*Z* or *trans*-to-*cis* transformation upon photoirradiation. The dihedral angle between aromatic/fused rings attached to the central double bond changes between ~90° and ~170° through structural isomerization, which depends on the size and structure of the rings [18–21].

Azobenzenes, one of the most widely studied classes of photoswitches, consist of two benzene rings connected via a central azo group. Generally, upon irradiation with UV light, this azo group is able to isomerize from *E* to *Z* conformation. The reverse process is triggered either through thermal activation or by visible light irradiation. Potential applications for azobenzenes in the solid state include photon energy storage [22–24] and nanoimprint lithography [25]. However, due to the large volume change required for switching, their isomerization has proved difficult in the solid state [26].

Hydrazones have only recently been exploited for their photoswitching properties by Aprahamian et al. Hydrazones can exhibit two thermodynamically stable isomeric forms, depending on the H-bond acceptors present in the molecule, both intra and intermolecularly [27,28], as well as *para* electron-withdrawing or electron-donating groups functionalized on the benzene ring [29]. One can therefore, by changing the H-bond acceptors, tune the E/Z ratio at equilibrium upon photoswitching, which is a vast improvement

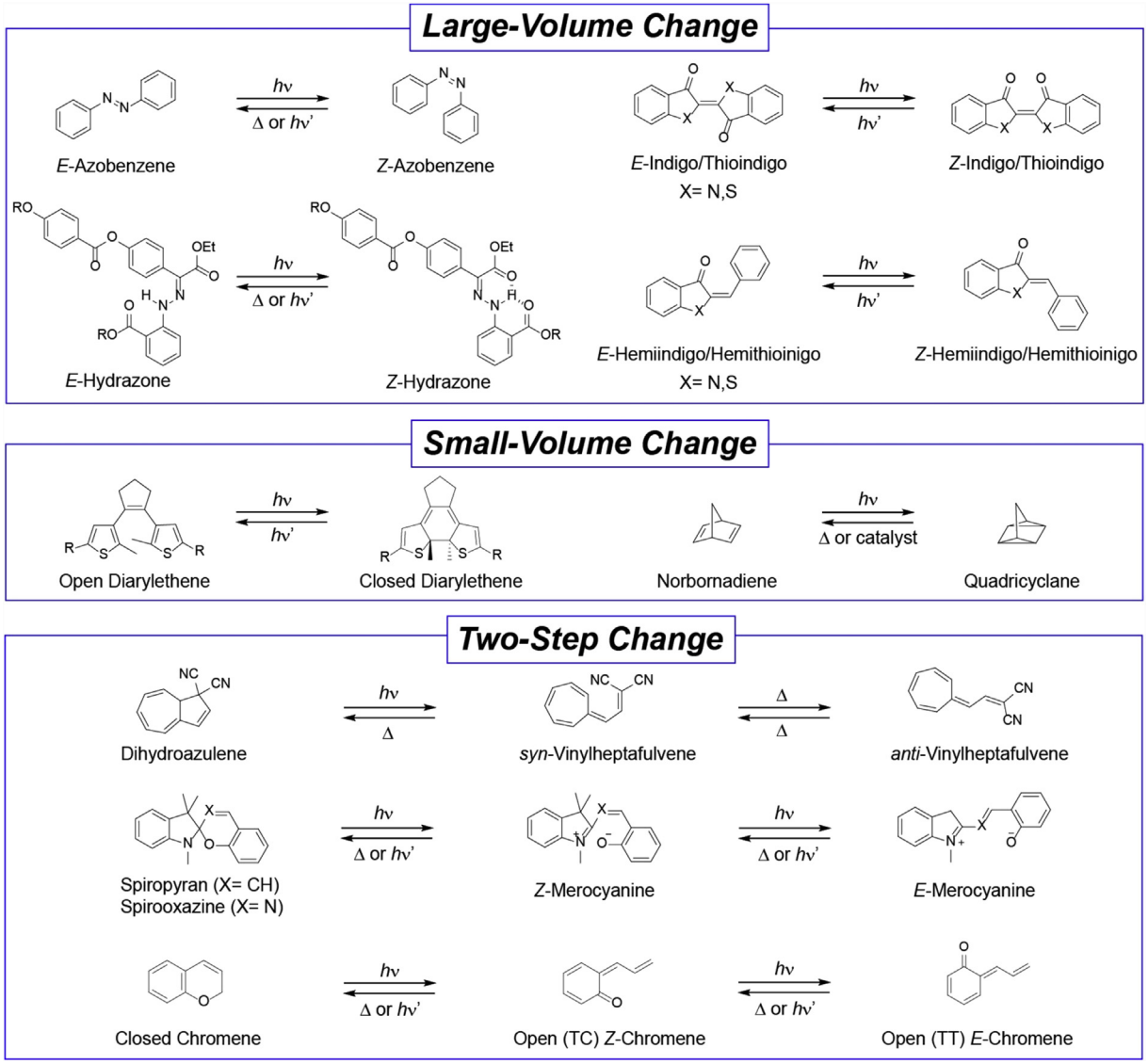

Scheme 1. General photoisomerization for common photochromic compounds.

from the original hydrazones that could only irreversibly photoswitch [30]. Common use of hydrazones is in liquid crystal networks/polymers, and, more broadly, for changing the macromolecular morphology. More information on hydrazones can be found in a recent review by Aprahamian [31].

Indigoids have been studied greatly by Dube et al. [32], and their *E*-to-*Z* isomerization can be carried out by visible light irradiation for both forward and reverse processes, which makes them attractive candidates for biological applications including photopharmacology. Isomerization occurs about the double bond connecting the hemiindigo/aryl groups. Many variations of indigoids exist, including indigos (X = N), thioindigos (X = S), hemiindigos (X = N), and hemithioindigos (X = S). Although indigoids have not been studied as extensively as the above-mentioned photoswitches, they do exhibit favorable characteristics such as high quantum yields (~56%) and thermal stability.

1.2. Photoswitches that require small volume change

Unlike azobenzenes, hydrazones, and indigoids, photoswitches including diarylethenes (DAE) and norbornadienes (NBD) isomerize through ring-opening or ring-closing process that requires smaller volume change.

DAEs involve two aryl groups connected by a central ethene group. Upon irradiation with UV light, the two aryl groups make a new covalent σ bond to form a central six-membered ring, which can be reversed upon visible light irradiation. Although this ring-closing behavior is accompanied by a slight decrease in length (~0.11 nm) along the horizontal axis, it results in a small increase in length (~0.07 nm) vertically [33]. More information about DAEs can be found in a review by Kobatake et al. [34] and other research papers [35].

NBD possesses a bridged bicyclic ring structure. Upon irradiation with UV light, the two π bonds undergo cycloaddition to form four σ bonds, leading to quadricyclane (QC) and a slight increase in volume due to the formation of an additional ring. The reverse transformation occurs via thermal activation or catalysis [36]. Studies have shown this compound as a promising candidate for solar energy storage in the liquid state as well as solid state by incorporating a polymer scaffold [37,38].

1.3. Photoswitches that undergo two-step isomerizations

While the molecules discussed so far exhibit one-step transformation, other molecules involve two-step isomerization that requires σ bond dissociation (i.e. ring-opening) followed by the rotation of a bond in the open form. Overall, the volume requirement for the isomerization is significant, similar to the switches shown in the first category.

1,8a-Dihydroazulene-1,1-dicarbonitrile (DHA) also undergoes two-step isomerization. When irradiated with UV light or treated by a strong Lewis acid, DHAs open up the cyclopentene unit to generate a conjugated diene structure named vinylheptafulvene (VHF). Upon ring-opening, VHF rapidly converts from its *syn* conformation to its thermodynamically stable *anti* form. The reverse isomerization steps are facilitated by thermal activation. Studies have shown that the mechanism for DHA-to-VHF photoswitching in solution involves a highly polar transition state [39] while the solid-state transition proceeds through a diradical intermediate [40]. Other studies indicated that ring closure proceeds through a zwitterionic transition state and DHA forms in two pairs of enantiomers, of which the ratio can be manipulated by solvent polarity [39].

Spiropyrans (SP) and spirooxazines (SO) photoisomerize from the closed neutral form to the open zwitterionic merocyanine (MC) form [41]. When irradiated with UV light, the C—O σ bond of SP and SO breaks to form the transient *Z* isomer of MC. This quickly converts to the more thermodynamically stable *E* form exhibiting a more linear structure [42,43]. The switching processes can be monitored by a color change from the colorless closed form to the blue/violet open form. Common uses for SP and SO are in optical storage/memory devices [44]. In addition, they are promising for biological applications due to their solubility in aqueous solutions [45]. Heckel et al. in particular have demonstrated successful photoswitching and incorporation of SP into oligonucleotides *in vitro* [46] as well as their low toxicity and resistance to hydrolysis in biological conditions [45]. A thorough review by Klajn highlights the SP-based dynamic materials, which provides more in-depth insight about the class of switches [47].

Chromenes exhibit ring-opening upon UV light irradiation through a short-lived *transoid-cis* (TC) form. The TC is thermally unstable and can either revert back to the closed-ring chromene or isomerize to its *transoid-trans* (TT) form depending on the respective activation energy. Both the TT and TC form can isomerize back to the closed form via visible light irradiation [48]. These forms, along with the open MC form of SP, are controllable through thermal activation based on studies done on isomerization dynamics at low temperatures, which will be further discussed in the next sections [49,50].

2. Isomerization dynamics in solid state: pristine switches

Unlike solution-state switching of molecules as widely studied and described in Scheme 1, switching in the solid state is difficult to observe due to the intermolecular stacking and the lack of free space, which limits conformational changes. In addition, metastable photoisomers generated in solid undergo rapid thermal reversion to ground-state isomers at room temperatures. In this section, we discuss examples of photoswitching observed in the solid state, despite low conversion rates, enabled by reducing temperature or by the processes that generate amorphous solid state of switches.

2.1. Low temperature studies

Evidence of photoisomerization of SP to MC in the solid state is limited. Similar to azobenzene, SP molecules pack closely in the condensed phase. Because SP switching requires a large structural change, steric hindrances obstruct effective switching.

In solid state, fast thermal reversion (MC-to-SP) results in a short lifetime of the MC isomer at ambient temperature [41]. This suggests that colorless SP crystals may be photoswitching to their colored MC forms in the solid state upon UV light irradiation; however, thermal isomerization significantly lowers the observable MC content, based on minimal photocoloration. Decreasing the temperature reduces the available energy for thermal reversion; therefore, at lower temperatures, photochromic SP **1a** and SO **1b** crystals exhibit spectral changes and enhanced photocoloration upon photoisomerization to MC isomers (Fig. 1) [43].

Chromenes encompass benzopyrans and naphthopyrans. A study on solid-state photochromism of microcrystalline powders over a temperature range between 80 K and 300 K reveals that various UV-induced isomers are responsible for the photochromic properties of chromenes [49]. Indeed, when the closed form is irradiated, the compound isomerizes to a *cisoid-cis* (CC) intermediate which rapidly converts to the TC form (Fig. 2a). The TC form is thermally unstable, observed only at low temperatures, as it can easily revert back to the closed form through rotation of the single bond (C_2—C_3). On the other hand, the TT form is more stable than

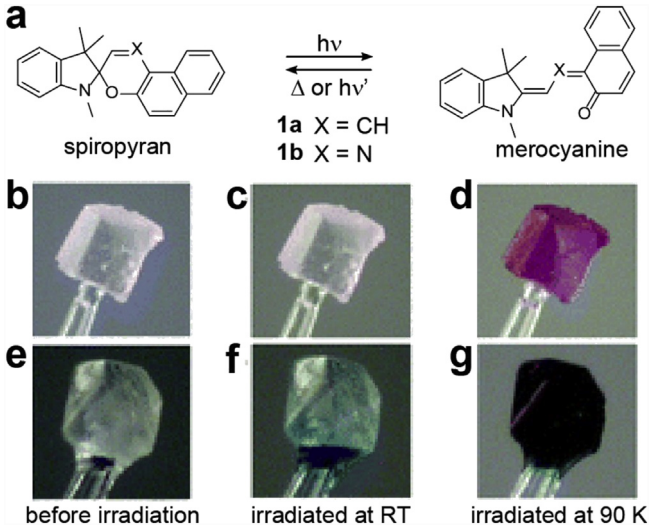

Fig. 1. (a) Schematic of photoisomerization of SP **1a** and SO **1b**. (b–g) Optical images of crystals of **1a (b, c, d)** and **1b (e, f, g)**, before irradiation (left), after irradiation at room temperature (center), and after irradiation at 90 K (right). Reproduced and adapted from Ref. [43] with permission from The Royal Society of Chemistry.

TC, requiring rotation of both the single (C_2–C_3) and double (C_1=C_2) bonds in order to revert back to the closed form.

Similar to SP crystals [41], color intensity increases for chromene crystals irradiated at 90 K. These colors are caused by the TC and TT forms, along with two unstable, nonplanar ring-opened species, believed to be *cisoid* isomers (Fig. 2b). The *cisoid* isomers, which are extremely short-lived in the solution state, were stable enough at 100 K in the solid state to be observed by steady-state spectroscopy only for compound **2a**. In order to observe TT at room temperature, it must first be formed by UV irradiation of the closed form to the TC form at low temperature followed by gentle heating. Both the TC and TT forms do not revert to the closed form upon irradiation with visible light at low temperatures, but rather form a colorless allenylnaphthol intermediate through a process similar to that of photobleaching of chromenes in solution (Fig. 2c). Gradual heating from 80 K to 200 K in the dark returned the photobleached allenylnaphthol intermediate of **2b** to the colored TC form [49].

To better understand fundamental photoisomerization mechanisms, studies were performed on hemithioindigo compound **3**, a photochromic compound with four different diastereomer forms (Fig. 3). These forms do not interconvert thermally at ambient temperature and therefore allow for observation and identification of primary photoproducts in restricted environments, including rigid matrices of solvent glasses or at very low temperatures. Based on photoswitching studies under 405-nm irradiation of atropisomers **3a** and **3b**, which are in the *Z*-state, in frozen solutions of toluene-d_8 and $CDCl_2$ at −196 °C, and diethyl ether/iso-pentane/ethanol glass at −183 °C, there is notable preference for the formation of the double bond isomerization products and, to a lesser extent, isomers obtained from the hula twist pathway. Overall, there is minimal isomerization between *Z* forms. This demonstrates that increasing viscosity of the surrounding environments has preference for isomerization between *Z* and *E* forms, although the specific mechanism followed depends on the solvent [51].

DHA-to-VHF isomerization, while facile in solution, is significantly more difficult to perform in the solid state. In solution, UV light irradiation of DHA induces isomerization to *syn*-VHF, which can then easily isomerize to the thermally stable *anti*-VHF. However, the large structural change that occurs from DHA to the thermally stable *anti*-VHF means it is inherently prohibitive in the solid state (Fig. 4a). This large structural change is in contrast to the formation of *syn*-VHF, which shows less structural change as seen by the fit in the stereoscopic drawing of the DHA cavity (Fig. 4b). Although the reaction to *syn*-VHF is more probable in the solid state, close packing, and therefore steric hindrance, still inhibits isomerization. As a result, the conversion of DHA to *syn*-VHF under UV irradiation is only 10% after 18 h under ambient conditions.

The use of two-photon excitation to increase isomerization in a single crystal revealed the closed-shell product, *syn*-VHF, via X-ray photodiffraction. UV excitation to *syn*-VHF allows switching while maintaining crystallinity because little change occurs to the unit cell. Back-reaction to DHA occurs rapidly upon heating to 298 K. In addition to isomerization through a closed-shell zwitterionic intermediate, the reaction also proceeds via a homolytic bond cleavage, which forms an open-shell diradical species that is stable below 160 K (Fig. 4c). Results from fluorescence decay indicate that at low temperature the reaction is dominated by the diradical mechanism, while above 298 K the diradical is less stable and hence *syn*-VHF is formed via the closed-shell intermediate. Furthermore,

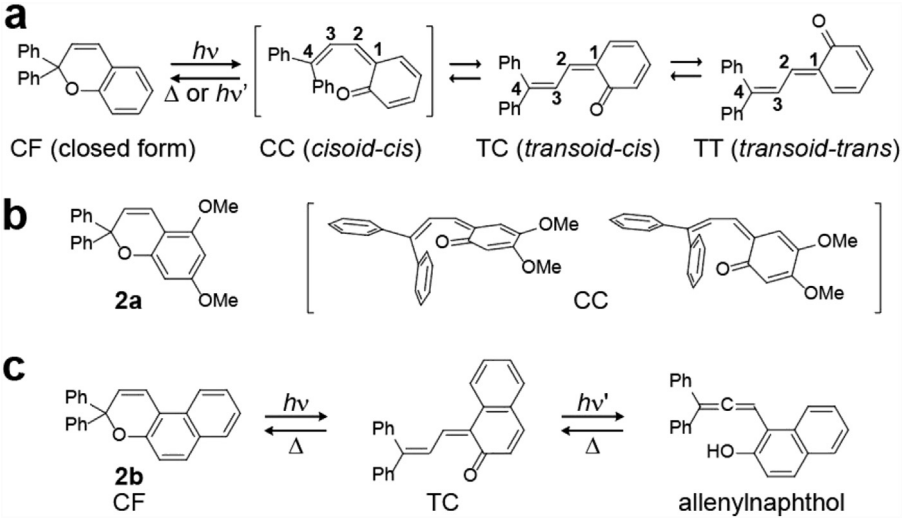

Fig. 2. (a) General isomerization of chromene from the closed form to open forms *cisoid-cis* (CC), *transoid-cis* (TC), and *transoid-trans* (TT). (b) Proposed nonplanar CC structures of **2a**. (c) Schematic showing isomerization of **2b** at 80 K between closed form and allenylnaphthol form.

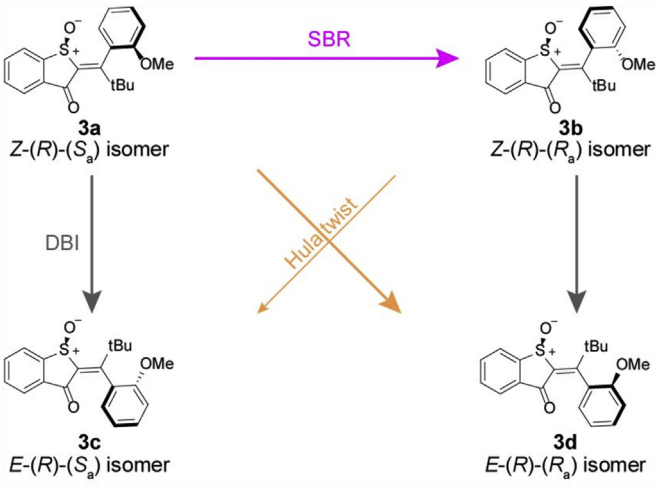

Fig. 3. Diastereomers of hemithioindigo compound. **3a** and **3b** are atropisomers of each other, and **3c** and **3d** are atropisomers of each other. SBR, single-bond rotation; DBI, double-bond isomerization.

variable-temperature Fourier-transform infrared spectrometry (Fig. 4d) shows that photoirradiation at 77 K causes two nitrile stretches at 2217 cm^{-1} and 2205 cm^{-1}. At 298 K, photoirradiation results in a single nitrile stretching band at 2217 cm^{-1} that does not split upon cooling to 77 K. This supports that the nitrile stretch at 2205 cm^{-1} is due to a diradical intermediate [52].

2.2. Room temperature studies

As a means to investigate kinetics of photoisomerization in the solid state, Garcia-Garibay et al. carried out nanosecond transient absorption spectroscopy experiments for the ring-opening photochemical mechanism of SP **5a** (Fig. 5a) in acetonitrile and within nanocrystals suspended in aqueous solution. The aqueous environments served to increase the probability of observing single excitation photoprocesses, whereas large single crystals and dry powders would have given rise to complex kinetics from multiphotonic interactions. Comparisons were made between **5a** in an acetonitrile solution and nanocrystals of **5a** suspended in water, the latter of which is intended to study kinetics in the solid state. Computed UV−vis spectra predicted intermediate MC-like structures for **5a**. The emergence of transient species allows for lattice disorder that ultimately creates the space to accommodate isomerization in the solid state whereby *E*-MC is eventually stabilized. Furthermore, the transient absorbance spectra did not show decay of the corresponding MC band between 550 and 650 nm at timescales of up to 4 ms, indicating that a stable *E*-like MC species is attainable in the crystalline environment, even when using a weaker laser pulse. Ultimately, nanocrystal suspensions provide a method of studying the kinetics of photochromic processes in the solid state by minimizing the probability of multiphoton processes [53].

Cationic pyrido-spiropyrans are a novel type of photoswitch that have been observed to exhibit more facile photochromism in the solid state compared to their neutral counterparts (Fig. 5b). Bulk samples for compound **5c** were determined by X-ray powder diffraction to undergo significant disorder of the crystal structure upon irradiation with UV light. The initial structure could not be recovered, and the positive charge on the pyridine N atom may be responsible for the increased stability of the MC form in the solid state. The anion has less of an influence on the observed photochromism, as similar results were observed when different counteranions were employed into the structures [54].

SP derivatives have demonstrated potential in optical information storage. Amorphous films derived from a melt-cooling process

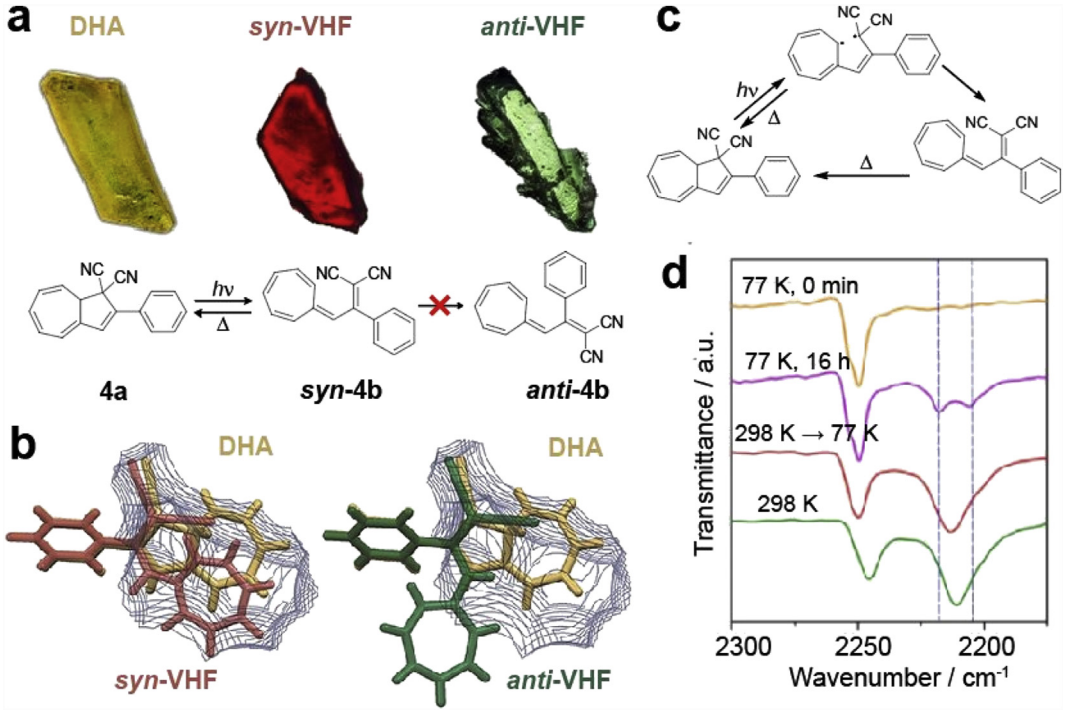

Fig. 4. (a) Crystals of DHA, *syn*-VHF, and *anti*-VHF with corresponding solid-state isomer structures. *Syn*-VHF was obtained from direct irradiation of a DHA crystal with UV light. *Anti*-VHF crystal was obtained by irradiation of DHA solution with UV light and subsequent crystallization below room temperature. (b) Predicted structures of *syn*-VHF (left) and *anti*-VHF (right) in the cavity of a stereoscopic drawing of DHA. (c) Reaction scheme for solid-state isomerization of DHA to *syn*-VHF via open-shell diradical intermediate. (d) Variable-temperature FT-IR spectra showing presence of nitrile stretches at 2217 cm^{-1} and 2205 cm^{-1} corresponding to *syn*-VHF and the diradical intermediate, respectively. Reproduced and adapted with permission from Ref. [52]. Copyright 2018 Wiley-VCH Verlag GmbH & Co. KGaA. DHA, 1,8a-dihydroazulene-1,1-dicarbonitrile; VHF, vinylheptafulvene; FT-IR, Fourier-transform infrared spectrometry.

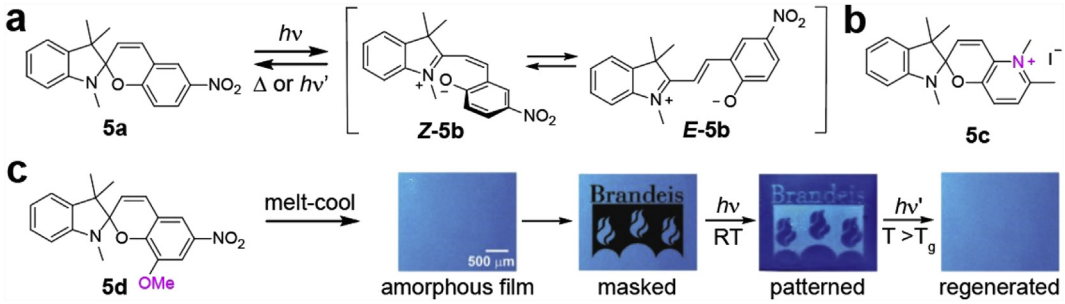

Fig. 5. (a) Proposed isomerization scheme between spiropyran **5a** and *E* and *Z* forms of **5b.** (b) Structure of cationic spiropyran **5c**. (c) Structure of methoxy-functionalized spiropyran **5d** and the process by which photoinduced patterning and subsequent pattern removal is performed for a melt-cooled amorphous film of **5d**. Reproduced and adapted from Ref. [55] with permission from The Royal Society of Chemistry.

show effective patterning when irradiated with UV light; the exposed regions on the film become darker as the MC content increases, despite less than ~1% conversion to MC. These patterns remain for weeks under ambient conditions, with regeneration of the original film induced by simultaneous heating above the glass transition temperature (T_g) and strong visible light irradiation (Fig. 5c). In contrary, patterning is difficult to achieve in the crystalline phase due to the lack of free space from close-packed structure, hindering isomerization from the closed SP form to the open MC form [55].

Photoswitching of DAE **6a** and **6b** were investigated in solid-state amorphous films (Fig. 6) prepared by cooling molten samples between two glass plates. The amorphous film composed of **6a** remained stable under ambient conditions; however, the film composed of **6b** was reported to crystallize in several days. Samples were irradiated with a Xe lamp at 330 nm for **6a** and 400 nm for **6b**. Compared to the photochromic reaction efficiencies in hexane solution, **6a** films possessed a relative cyclization efficiency of 0.49, whereas the crystalline films of **6b** did not exhibit any photochromism. However, the amorphous film of **6b** was observed to immediately turn purple upon UV irradiation, although its relative cyclization efficiency was only 0.03 compared to the hexane solution. Cyclization is more effective in amorphous films than polycrystalline films; however, isomerization in the solid state remains less effective compared to hexane solutions. Inefficiency supports that packing structure of the condensed phase influences photoswitching of DAE between open and closed forms [56].

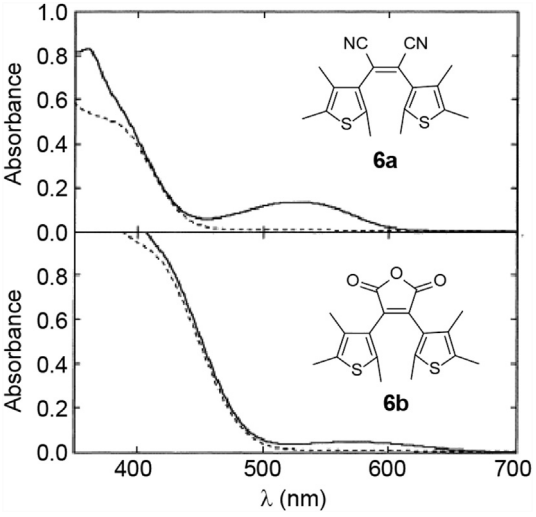

Fig. 6. Structures of DAE derivatives **6a** and **6b** and the respective absorption spectrum in amorphous films before (dashed line) and after (solid line) UV irradiation. Reproduced and adapted from Ref. [56]. Copyright 1999 Elsevier Science S.A. DAE, diarylethenes.

3. Strategies for facilitating solid-state photoswitching: functionalization methods

3.1. Covalent functionalization of small molecules

In order to achieve facile photoswitching of small molecules in the solid state, creative strategies were employed in the functionalization of these compounds, inducing out-of-plane distortion, increasing bulkiness of substituents, and incorporating switches as auxiliary ligands of transition metal complexes (Table 1). Small-molecule photoswitches in the solid state prove to fit a multitude of applications, including photon energy storage, gas adsorption, and photomechanical bending, to name a few.

A simple approach to increasing the free volume of azobenzene molecules in the solid state is functionalization with bulky groups (Fig. 7a), particularly aromatic groups, which breaks the planarity of molecules and prevents their crystallization. As a result, amorphous and uniform films that can cycle between UV and visible light irradiation or thermal reversion were achieved (Fig. 7b). The decrease in planarity of the molecule correlates to increasing free volume available for isomerization. In addition to inducing the disorder of azobenzene films, bulky functional groups also increase the internal steric hindrance of *cis* metastable isomers compared to *trans* ground state, in turn, increasing the energy difference between *cis* and *trans* states (ΔH). This is an appealing characteristic for solar thermal fuels (STFs) that store photon energy in strained chemical bonds and release it in the form of thermal energy [24].

Another approach to increasing the free volume in the solid state is by binding four azobenzene molecules to a central carbon atom, creating a three-dimensional tetramer (Fig. 8a). The arrangement of the tetramers features enough free volume for successful photoisomerization; upon *trans-cis* isomerization, thin films change from a porous, crystalline solid phase to a nonporous, amorphous phase. Furthermore, functionalizing at the *para* positions of the phenyl moieties with alkyl groups increased the porosity of the *trans*-phase. Compared to the unsubstituted tetramer **8a**, both **8b** and **8c** were able to selectively adsorb CO_2 from an N_2 environment in the entirely *trans* (E_4) form [57].

A metal complex with an auxiliary photoreactive ligand, cyanoethyl, axial to 4-aminoazobenzene ligand shows an improved photoisomerization in the solid state (Fig. 9). Upon irradiation of powder **9** with UV light, the cyanoethyl ligand changes conformation first from the β to α conformation, increasing the unit-cell volume enough to allow *trans-cis* isomerization of azobenzene ligand. The *cis* isomer reverts to *trans* after 24 h in the dark, without

Table 1
Photoswitch classes and their derivative Structures.

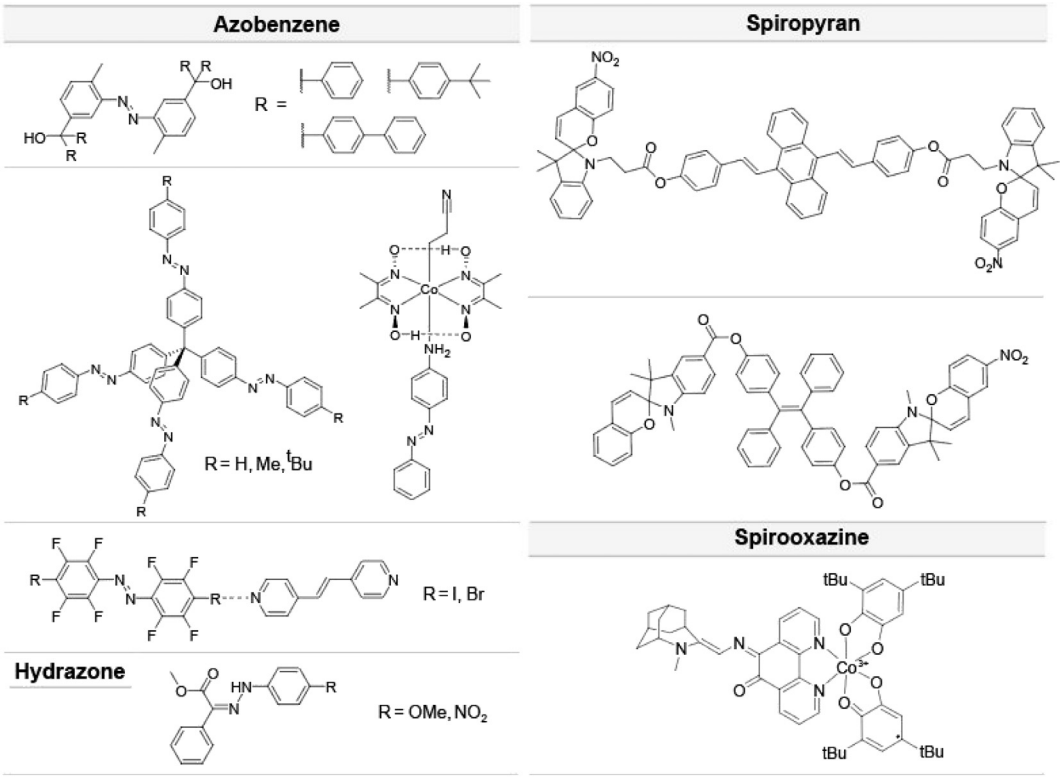

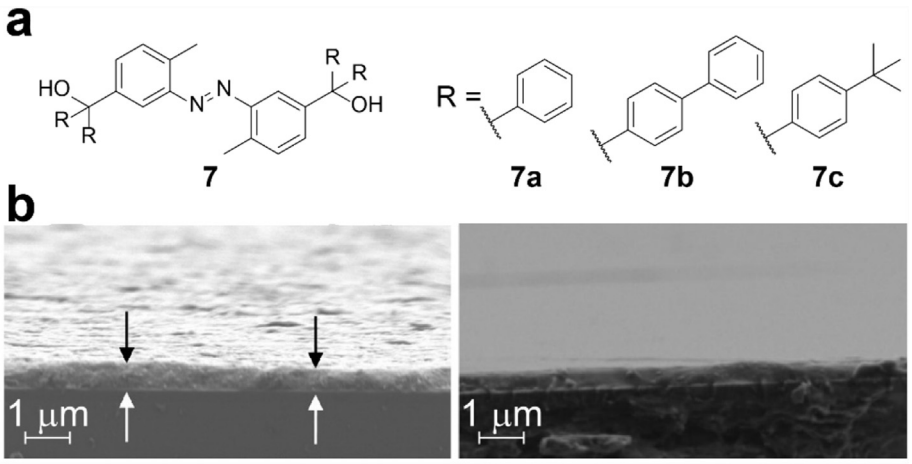

Fig. 7. (a) Azobenzene derivatives **7a-7c** with bulky, aromatic R groups. (b) Cross-sectional SEM of compounds **7a** (left) and **7b** (right). Arrows indicate the thin film's cross-section. Adapted with permission from Ref. [24]. Copyright 2017 American Chemical Society. SEM, scanning electron microscopy.

changes to the cyanoethyl ligand. For the first time, application of an auxiliary, photoreactive ligand has been shown to enable photoswitching of azobenzenes in the solid state, demonstrating a design strategy for solid-state photochromism through controlling crystal environment [58].

Friščić et al. reported irreversible crystal-to-crystal *cis-trans* isomerization of perhalogenated azobenzene **10a** (Fig. 10a), demonstrating permanent modification of a crystal through visible light irradiation (Fig. 10b) which results in highly controllable photomechanical bending. The transition occurs upon irradiation under 457-nm laser light; single crystal *cis* is transformed into a polycrystalline sample of *trans*. Perhalogenation stabilizes the *cis* form of azobenzene, which is inherently hard to isolate in its crystal state. Normally, the half-life of non-halogenated *cis*-azobenzene derivatives is very brief, ranging from seconds to minutes. Perhalogenation increases the half-lives to approximately two months, allowing accumulation of the *cis* form required for bending. Irradiation of a crystal of *cis*-**10a** resulted in irreversible bending, and by controlling the direction of irradiation, the direction of photomechanical bending was controlled [59].

A follow-up report by Friščić et al. discusses a co-crystallization strategy to investigate, for the first time, single crystal *cis-trans*

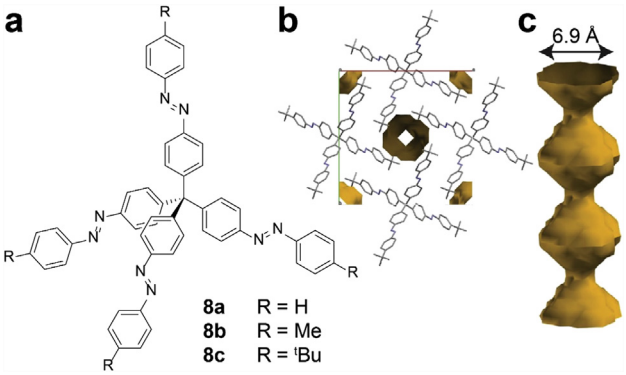

Fig. 8. (a) Star-shaped azobenzene tetramer with hydrogen or alkyl functional groups at R. (b) Crystalline arrangement of the tetramers **8c**, in an all-*trans* (E_4) conformation, with a porous channel segment at its center. (c) Side view of a porous channel segment. Reproduced and adapted from Ref. [57] with permission from Springer Nature.

isomerization of azobenzene through *in situ* X-ray diffraction. This new approach overcomes many limitations regarding the study and design of azobenzene crystals, such as chromophore variety, synthesis of chromophores, and crystal morphology, as well as difficulty isolating the *cis* form due to the short half-life. Cocrystals were made using an electron-deficient perfluorinated azobenzene, with highly polarizable iodine acting as the halogen bond donor, and azo- or olefin-based pyridine derivatives (i.e. bpe) as halogen bond acceptors (Fig. 10c). Using single-crystal XRD, (*cis*-**10b**)(*cis*-**bpe**) was transformed to (*trans*-**10b**)(*cis*-**bpe**) at 532-nm irradiation at 5 mW/cm at 298 K over the course of 3 h (Fig. 10d). Furthermore, by repeating this irradiation with 15 mW/cm at 200 K (presumably to hinder recrystallization) over the course of 1 h, the diffraction pattern disappears, revealing that *cis-trans* isomerization of perfluorinated azobenzene cocrystals undergo an amorphous phase before recrystallization [60].

Recently, a hydrazone-based photoswitch featuring robustness, bistability, facile synthesis, and functionality in the solid state was synthesized by Aprahamian et al. (Fig. 11a). The *E* isomer as a solid-state film did not exhibit changes in the absorption spectrum after one month at room temperature, indicating remarkable thermal stability. Photoswitching between visible light and UV or heat enables switching between the *E* and *Z* forms, respectively [61]. In UV–vis cycling experiments where photoswitching of films was performed with alternating wavelengths of 360 nm and 450 nm, emission intensity was found to decrease in the first cycle, but remains stable over subsequent cycles. This may be attributed to an annealing effect in which the crystalline *Z*-isomer reorganizes within the film during the first cycle. The film isomerizes when irradiated with high-intensity blue light (430–470 nm), undergoing a phase transition from the crystalline state to an amorphous state, as evidenced by the disappearance of optical birefringence and fluorescence emission. Along with facile synthesis, high fatigue resistance, reversibility, and fluorescence switching in the solid state, this type of photoswitch is highly desirable as a multifunctional material [62]. Further studies on hydrazones functionalized with electron-donating or electron-withdrawing groups reveal the importance of free space for successful solid-state photoswitching (Fig. 11b). Thin films of hydrazones functionalized with electron-donating groups were able to switch due to the loose-packed arrangement influenced by the rotary phenyl group shifting out of the plane (Fig. 11c), whereas electron-withdrawing groups directed the hydrazones to pack in a head-to-tail arrangement, minimizing the space available for switching to occur, if at all (Fig. 11d) [63].

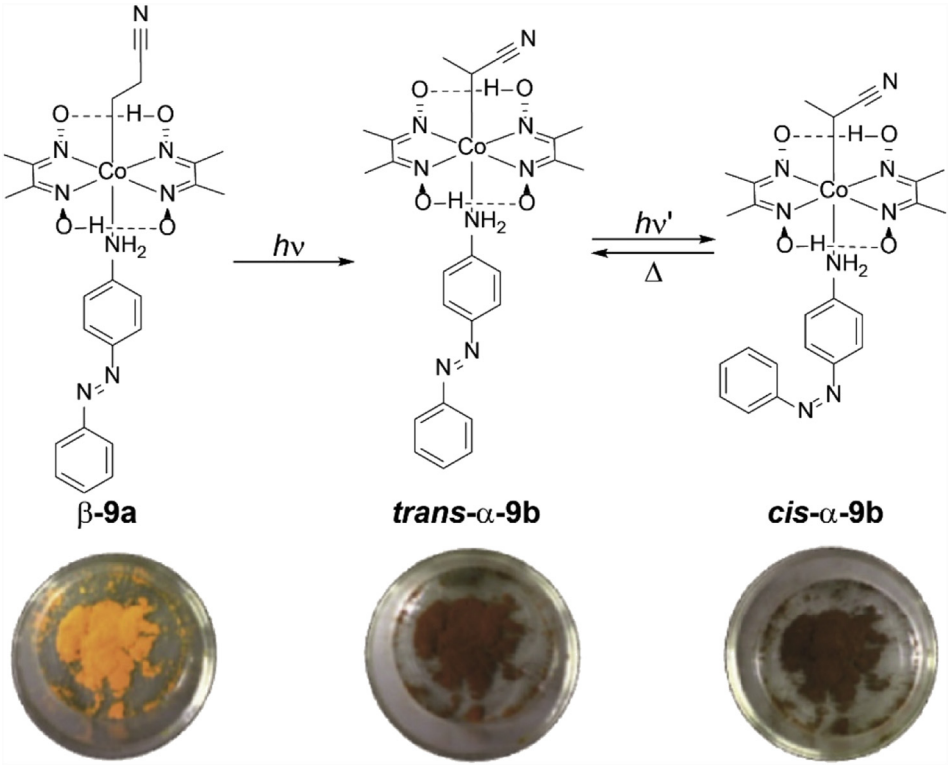

Fig. 9. Isomerization scheme of **9** (top) and corresponding compounds as powders (bottom). Reproduced and adapted with permission from Ref. [58]. Copyright 2012 The Chemical Society of Japan.

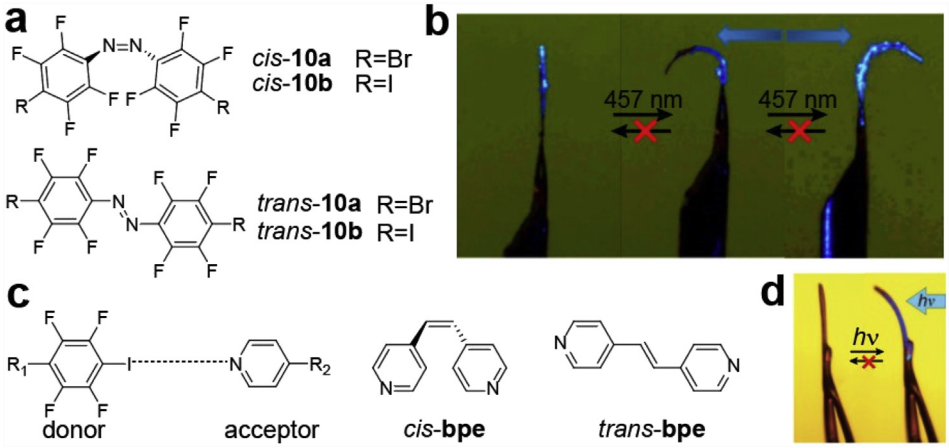

Fig. 10. (a) *cis* and *trans* forms of **10a** and **10b**. (b) Irreversible bending of a thin crystal of **10a** by 457-nm light, with blue arrows indicating direction of irradiation. Adapted with permission from Ref. [59]. Copyright 2013 American Chemical Society. (c) *cis* and *trans* forms of **bpe**, the electron acceptor that cocrystallizes with the **10b** donor. (d) Irreversible photomechanical change in shape of (*cis*-**10b**)(*cis*-**bpe**) upon irradiation to (*trans*-**10b**)(*cis*-**bpe**), with the blue arrow indicating the direction of irradiation. Reproduced and adapted from Ref. [60] with permission from The Royal Society of Chemistry.

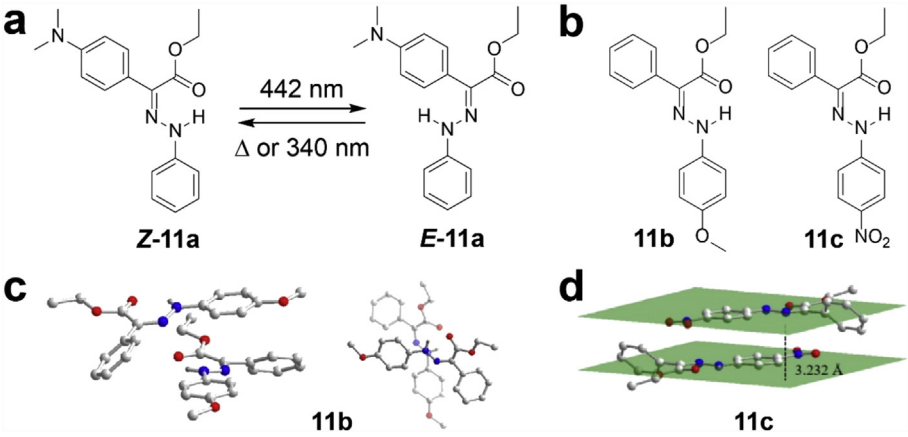

Fig. 11. (a) Isomerization of hydrazone structure **11** between *Z* and *E* forms. (b) Structures of hydrazones **11b** and **11c**. (c) Packing between two molecules of **11b** in the solid state (left) and top view of the packing in **11b** (right). (d) Crystal packing of **11c** showing a distance of 3.232 Å between two hydrazone backbones, encompassed by the green planes. Adapted with permission from Ref. [63]. Copyright 2019 American Chemical Society.

Approaches to employ SP in the solid state include the covalent linkage of SP units to aggregation-induced-emission molecules. These are π-conjugated luminescent structures that take on highly twisted conformations, avoiding intermolecular π-π stacking. The aggregation-induced-emission moiety serves to increase the free volume and promote solid-state photoswitching, resulting in compounds that easily and reversibly isomerize in the solid state, both as powders and as thin films, upon exposure to alternating UV and visible light irradiation. Furthermore, the MC forms of these molecules exhibited longer thermal lifetimes in the solid state compared to the solution state, indicating increased stabilization from a decrease in the vibrational and rotational freedom within the solid [64,65].

A novel system that induces magnetization switching of paramagnetic complexes through photochromic SO ligands was introduced by Frank et al. This system is unique in that magnetization is not only switchable in solid-state thin films, but that the photomagnetic states possess long lifetimes at temperatures above 300 K. Previous efforts to induce photomagnetic states based on ligand-driven spin-crossover processes were performed in solutions, and solid-state switching was only achieved at temperatures below 200 K. The authors describe the generation of photomagnetic states as a photoisomerization-induced spin-charge excited state process (Fig. 12), in which the lifetime of the magnetization state is dictated by the lifetime of the photochromic ligand state. The lifetime of the closed form SO ligand is in the order of seconds, whereas magnetization induced by the direct excitation of the metal-centered excited states only lasts for a few nanoseconds [13].

3.2. Covalent functionalization of polymers

Poly (methyl methacrylate) (PMMA) is a common backbone functionalized with photoswitches, particularly azobenzenes (see Table 2). A solid-state solar thermal fuel material was achieved by the facile synthesis of an azobenzene-functionalized PMMA (Fig. 13a). The polymer is soluble in many organic solvents, making it easy to process into amorphous thin films. Heat release from the multilayered films during *cis*-to-*trans* thermal reversion was imaged using an infrared camera (Fig. 13b). The polymer was also cross-linked by poly(ethylene glycol) diacrylate (PGda), to increase the film thickness by stacking layers, although at the cost of the gravimetric density [22]. Similarly, another example of a PMMA polymer incorporating azobenzene side groups is shown in Fig. 13c.

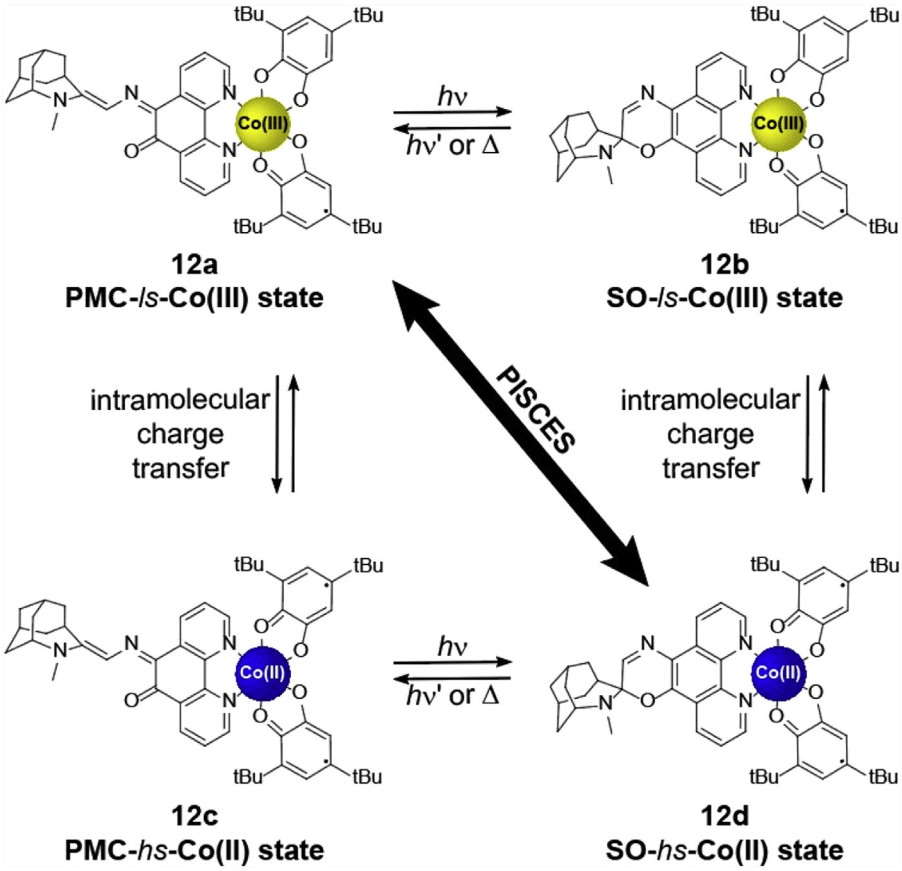

Fig. 12. Magnetization switching of paramagnetic cobalt complex through photoisomerization of spirooxazine (SO)-photomerocyanine (PMC) ligand. Adapted with permission from Ref. [13]. Copyright 2018 American Chemical Society.

In comparison to the unbound counterpart, these azobenzenes are not as closely packed in the solid state, yet π-π stacking contributes to hindered isomerization. To overcome π-π stacking interactions between the photoswitching moieties, methoxy groups were added to the four *ortho* positions on the azobenzene phenyl rings, forming PmAzo **13b** (Fig. 13c). *Ortho*-functionalization also led to a bathochromic shift of the *trans*-*cis* irradiation wavelength from UV light to blue light, eliminating the use of UV light which has the potential to decay molecules. Amorphous films of **13b** were able to take on patterns that were erased with visible light (Fig. 13d). The patterns were retained when films were stored in the dark at room temperature for 32 weeks. The long-term optical contrast of the photopattern is due to a lack of overlap of the n-π* bands between the *cis*-**13b** and *trans*-**13b** [66].

Wu et al. have shown that, by controlling glass transition temperature (T_g) through switching between *cis* and *trans* isomers, azopolymers with either PMMA or poly(methyl acrylate) backbones can be reversibly switched between solid and liquid phases (Fig. 13e and f) [67]. For azopolymers **13c-13f**, the *trans* isomer possessed a high T_g above room temperature, whereas a low T_g below room temperature was characteristic of the *cis* isomers. According to differential scanning calorimetry (DSC) measurements for **13c**, the T_g is −10 °C for the *cis* isomer and 48 °C for the *trans* isomer. Under alternating UV and visible light irradiation, **13c** was shown to undergo complete reversible isomerization for at least five cycles.

SP has been employed as a side chain unit in a polyimide to increase the thermal stability of the structure for high-performance multifunctional memory devices. It was observed that polymer-bound SP units possess improved reversibility and fatigue resistance upon alternating UV and visible light irradiation when compared to the unbound form doped in a PMMA polymer matrix. It is important to note that the MC moieties experience slower ring closure than ring-opening, demonstrating that the steric hindrance induced by the polyimide backbone may be important in stabilizing the MC form in the solid state [68].

Romdhane et al. previously employed NBD in a polymer system and investigated the system's photochemical properties [69]. It was expected that through pentamethylation, which would introduce bulk and a decreased polarity to the polymer structures, there would be improvements in solubility, film-formation, and photochemical valence isomerization. Indeed, following the synthesis of these derivatives, it was observed that NBD-to-QC photoswitching in a solid-state film could be promoted under sunlight irradiation. The thermal energy released during back conversion was studied by DSC measurement of irradiated polymer films as a potential system for STFs. In addition, the kinetics were found to be first order, and a 90%–95% conversion efficiency was achieved without side reactions. The lack of polymerization side reactions was attributed to steric hindrance from the addition of methyl groups. Along with the presence of a consistent exothermic peak for the conversion of QC to NBD, measured to be around 91–95 kJ/mol, the polymer maintained a consistent glass transition temperature (T_g) through multiple heating cycles, demonstrating that no side polymerization reactions occur, as well as the cyclability of heat release.

3.3. Incorporation to templates

Templating photoswitches can offer three key advantages, which involves controlling the arrangement of the photoswitching

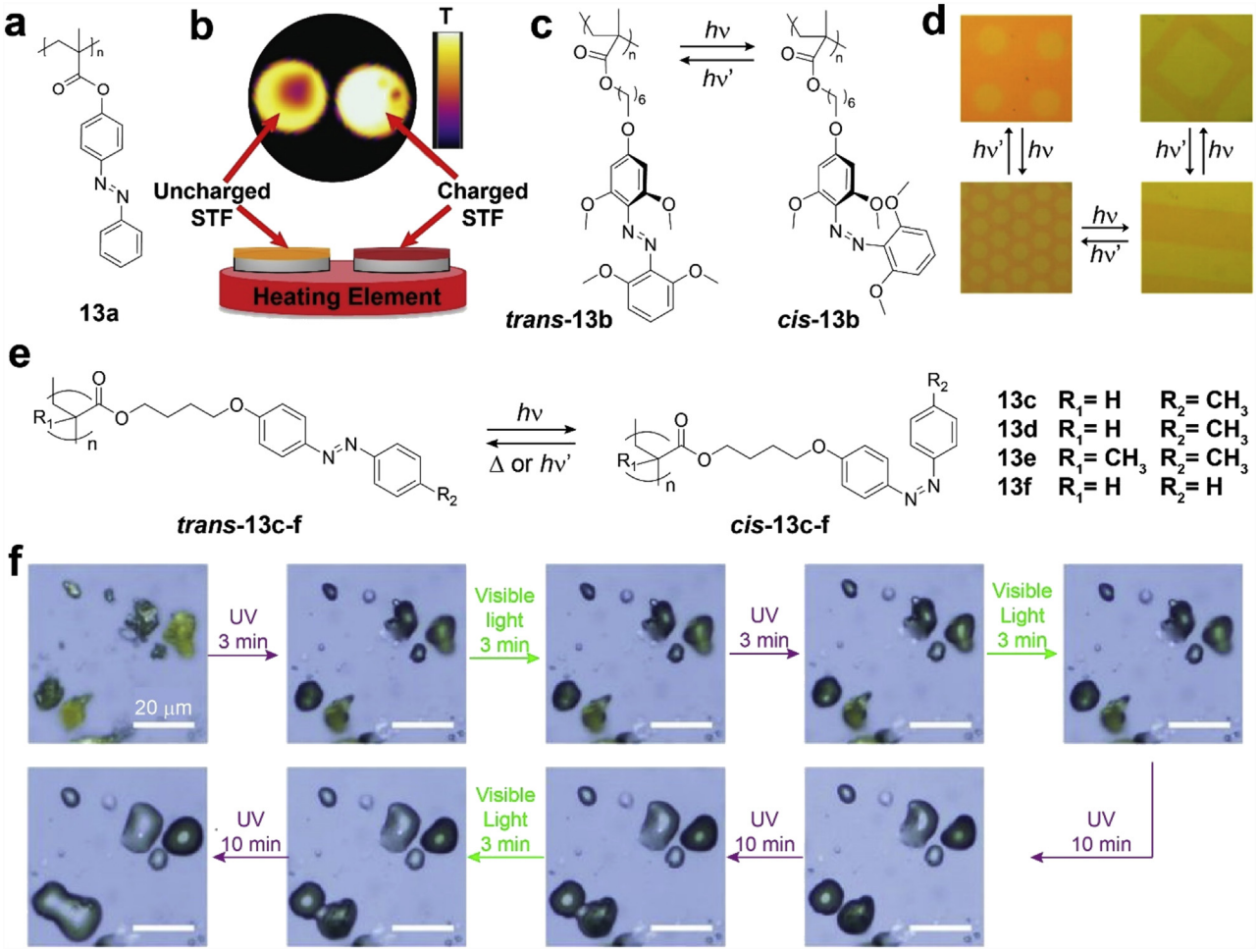

Fig. 13. (a) Structure of azopolymer composed of azobenzene side groups and PMMA backbone. (b) Experimental setup for determining heat release of charged films by infrared camera. Reproduced and adapted with permission from Ref. [22]. Copyright 2018 Wiley-VCH Verlag GmbH & Co. KGaA. (c) Reversible azopolymer isomerization scheme under different wavelengths visible light (625 nm and 470 nm). (d) Different photopatterns obtained by irradiation of azopolymer film. Adapted with permission from Ref. [66]. Copyright 2016 American Chemical Society (e) Reversible isomerization scheme between *trans* and *cis* forms of **13c-13f**. (f) Alternating UV and visible light irradiation on crystals of **13c**. Reproduced and adapted from Ref. [67] with permission from Springer Nature. PMMA, poly (methyl methacrylate).

moieties, providing enough space in which photoswitching can occur, and tuning photoswitching properties through electronic effects. This section describes three different kinds of templates: porous templates, particles as templates, and host-guest templates (Table 3).

3.3.1. *Porous platforms*

In order to improve the energy storage density of solid-state photoswitches for STF application, Grossman et al. developed another type of functionalized azobenzene system in which several photoswitching molecules are covalently bound to a rigid single-wall carbon nanotube (SWCNT) scaffold. Unlike their unbound counterparts, azobenzene molecules on the rigid scaffold experience different local environments based on density and steric interactions, ultimately influencing photoswitching properties. In the solid state, Azo-SWCNTs experience "bundling," in which azobenzene molecules of one scaffold interact with azobenzene molecules of an adjacent scaffold, effectively increasing the functionalization density by a factor of two (Fig. 14a). This introduces additional steric strain, further increasing energy storage density per azobenzene moiety by nearly 200% when compared to their unbound counterpart [23].

As a demonstration of solid-state STF applications, Luo et al. covalently functionalized SWCNTs with push-pull azobenzenes. The push-pull electronic structure increases the isomerization enthalpy, serving to increase energy storage density, with gravimetric density of the Azo-SWCNT-based films reaching 60.4 Wh/kg, approximately 50% more than that of the free azobenzene derivative (39 Wh/kg). These films remain stable under several irradiation cycles and are shown to possess an energy storage efficiency of 12.4%, showing potential as materials for high-energy, short-term STFs [70].

Imidazole-containing azoheteroarene (i-Azo-h) molecules grafted onto reduced graphene oxide (rGO) serves as potential material for photothermal batteries (Fig. 14b). The i-Azo-h/rGO films and powders were shown to have high power density (2380 W/kg and 3280 W/kg, respectively) due to a high-yielding *E-Z* isomerization (77.2%) and fast *Z-E* back-isomerization rate (6.1×10^{-3} s^{-1}) under green light irradiation at 535 nm. Reaction rate is influenced by favorable discharging due to intramolecular push-pull electronic structure. This material was applied to an information coding/encoding display employing thermochromic inks. In addition, upon irradiation with green light, the film releases heat fast, reaching ΔT of 3.3 °C within a minute, providing a material that can function under mild conditions [71].

Table 2
Photoswitch-functionalized polymers.

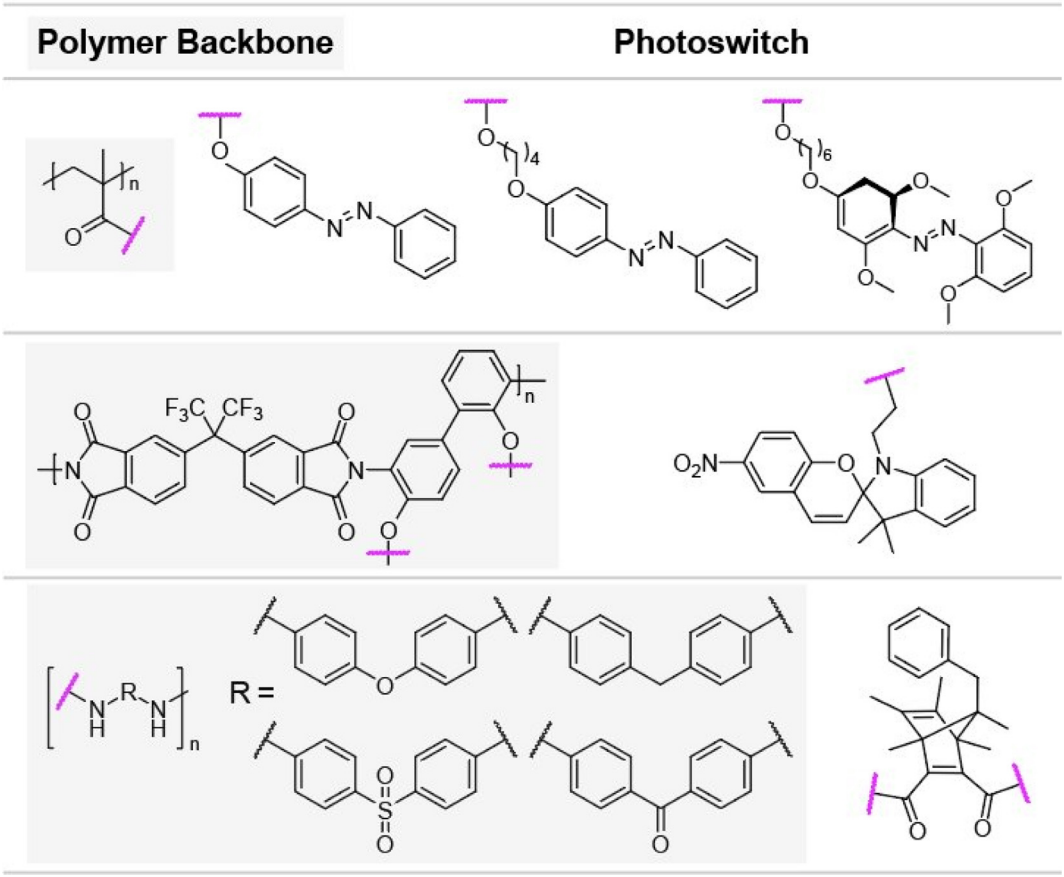

Table 3
Photoswitch-functionalized templates.

Template		Photoswitch
Porous platform	Single-walled carbon nanotube reduced graphene oxide	Azobenzene
	Dendritic fibrous nanoporous silica metal-organic frameworks $[Fe^{II}Fe^{III}(dto)_3]$	Spiropyran
Particle	Iron oxide, iron platinum	Azobenzene
	Polystyrene, Polyoxometalate	Spiropyran
Host-guest system	Polyimidazole-Pd cage complex	Azobenzene
	γ-Cyclodextrin	Spiropyran
	$[Ru(bpy)_3]^{2+}$(8-crown-ether)$_2$	Diarylethene

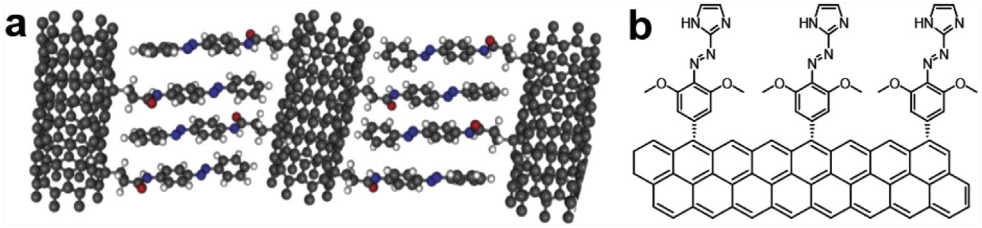

Fig. 14. (a) Image depicting Azo-SWCNTs bundling in the solid state. Reproduced and adapted from Ref. [23] with permission from Springer Nature. (b) Structure of the i-Azo-h/rGO system. SWCNTs, single-wall carbon nanotubes.

Another approach to improving the stability of the MC isomer in the solid state is by creating an environment that stabilizes both the uncharged and charged SP/MC isomers. A hybrid system consisting of a mixture of organophilic clay and mesoporous silica has been shown to stabilize both the SP and MC forms in the solid state, along with improving the switchability upon visible light discoloration and thermal coloration (Fig. 15). The zwitterionic MC isomer was stabilized by the

hydrophilic nature of mesoporous dendritic fibrous nanosilica (DFNS) [72].

Metal-organic frameworks (MOFs) as templates for photoswitches have been recognized as potential photoresponsive sensors. Photoswitches such as azobenzene, SP, and DAE have been incorporated into MOFs as linkers of the framework or as guests embedded into the pores [73]. SP molecules normally exhibit poor switchability in the solid state, but having pyridyl groups on both ends enables the SP unit to be spatially separated within the rigid MOF structure for solid-state switching. Pyridyl groups coordinate to the Zn metal centers in the MOFs (Fig. 16a). Linker (**16a**) incorporating SP molecule exhibits photoisomerization similar to free SP in the solution state, both under UV and visible light irradiation. This behavior indicates isomerization improves when SP molecules have sufficient free volume to change between open and closed forms. Another linker (**16b**) composed of two SP molecules shows lack of reversibility when embedded in MOFs due to the close packing arrangement of the two photoswitching moieties on each linker. Neither **16a** nor **16b** linkers were able to photoisomerize under UV irradiation in the solid state (Fig. 16b), corroborating that steric hindrance is a major issue for the photoswitching of SP molecules in the solid state [15].

A mixed Fe(II)/Fe(III) dithiooxalato(dto)-bridged bimetal complex system (Fig. 17a) creates a two-dimensional honeycomb network in which isomerization of the intercalated SP cations has been implied to control the system's magnetic properties. A combination of Fe(II) and Fe(III) was used because the reversible thermally induced charge transfer minimizes free energy in the system. The charge transfer phase transition and ferromagnetism of the 2D honeycomb network is influenced by the size of the intercalated cation, so by employing photoswitchable cationic SP molecules the size—and therefore the electronic and magnetic properties—can be controlled. Photoisomerization by UV irradiation has been shown to occur both at 70 K (Fig. 17b) and at room temperature, with the latter suppressing charge transfer phase transition and resulting in two ferromagnetic phases, one with a Curie temperature at 5 K corresponding to a low transfer phase and another at 22 K corresponding to high transfer phase [74].

3.3.2. Particles

Einaga et al. synthesized FePt nanoparticles coated with azobenzene molecules, which create a system in which magnetic properties are influenced by the changes in the electronic interactions between azobenzene ligands and the nanoparticle cores induced by photoswitching of the azobenzene molecules; particularly the changes are in the electronic polarization of iron d electrons covalently bound to the carboxylate groups of functionalized azobenzene ligands. This is supported by earlier work from the same group, which synthesized γ-Fe_2O_3 composite nanoparticles with covalently bound azobenzene ligands for similar purposes [75,76]. In both cases, photoisomerization is improved when *n*-octylamine was implemented as spacer ligands, increasing the free volume between photoswitches in solid state. Photoswitching the azobenzene moieties of the FePt nanoparticles achieved ferromagnetism at room temperature [77] (see Fig. 18).

Another approach to solid-state photoswitching uses polystyrene-based microparticles as a template for SP functionalization (Fig. 19, **19g, h**). By comparing electronic and kinetic properties with those of its unbound form (**19a, b**), one can study the impact of solid-state environment on these properties. Progressing across solution (toluene), dispersion (toluene/polystyrene), and solid (polystyrene matrix) states, isomerization of SP to the MC form becomes increasingly restricted for both microparticle-bound and unbound SP molecules, while the degree of restriction was more significant for the unbound system [78].

Another type of hybrid material, developed from the combination of SP/SO molecules and polyoxometalate (POM) systems (Fig. 20), enables excellent solid-state photoswitching at ambient

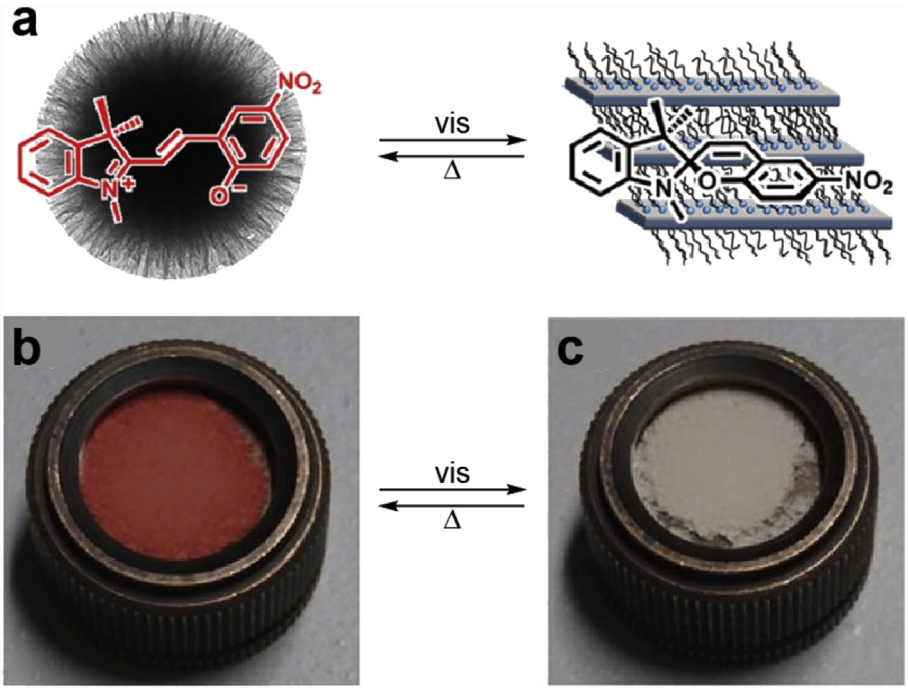

Fig. 15. (a) Scheme for photoswitching SP hybrid system. Photographs of DFNS/MC (high concentration) hybrids before (b) and after (c) visible light irradiation for 2 min. Thermal reversion of the samples took place in the dark at room temperature. Adapted with permission from Ref. [72]. Copyright 2018 American Chemical Society. SP, spiropyrans; DFNS, dendritic fibrous nanosilica; MC, merocyanine,

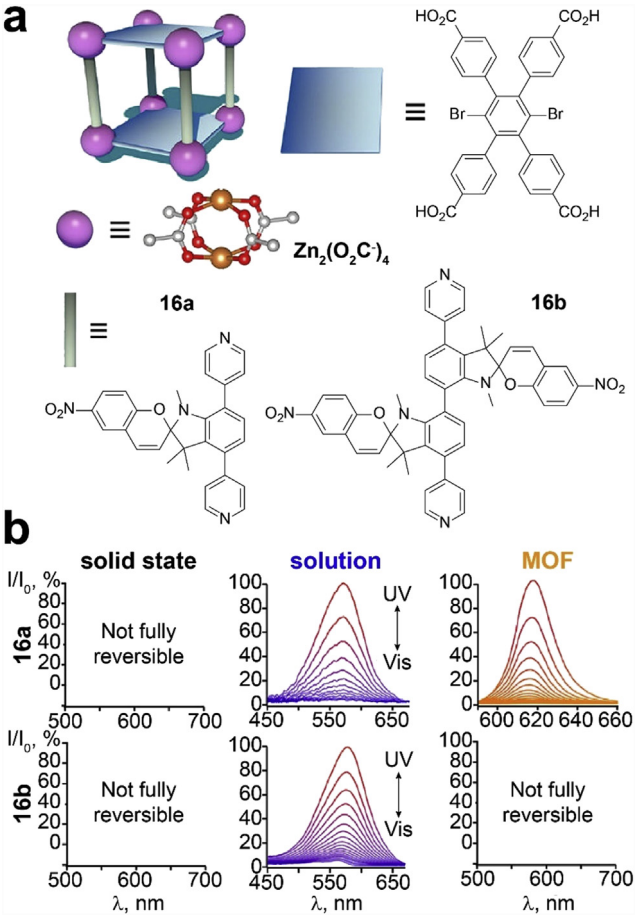

Fig. 16. (a) Scheme showing components of the MOF with photoswitching linkers **16a** and **16b**. (b) Normalized absorption plots for **16a** and **16b** in solid state, solution, and coordinated in the MOF. Adapted with permission from Ref. [15]. Copyright 2018 American Chemical Society. MOF, Metal-organic framework.

conditions, despite the geometrical constraints experienced by close packing between the photoswitches and the POM units. Due to the isostructural properties of the Mo-POM and W-POM anions, electronic factors were studied without changing the overall structure of the system. It was shown that W-based POMs improve solid-state photoswitching as a result of a better separation of absorption energies between the organic and inorganic moieties compared to its Mo-based counterpart, where Mo competes with the photochromic moieties for absorption of UV light. Further improvements to solid-state photochromism are due to the polar nature of the POM frameworks which stabilizes the zwitterionic MC form. This demonstrates that electronic factors also impact photoisomerization of the SP/POM and SO/POM systems [79].

3.3.3. *Host-guest systems*

Klajn et al. have demonstrated a cage system to allow solid-state photoisomerization of azobenzene [80]. Pristine azobenzene and *ortho*-tetrafluoro-azobenzene derivative **21b** (Fig. 21) were encapsulated within a polyimidazole-Pd cage complex in water, where azobenzene is normally insoluble. Two equivalents of *trans*-**21b** were able to enter and remain within the cage (Fig. 21b). Upon UV irradiation, one equivalent converts to *cis*-**21b** which forms an unstable heterodimer with the *trans* isomer. *cis*-**21b** is immediately expelled and enters a free cage in solution (Fig. 21c). Changes in color during photoisomerization inspired the investigation of light-induced patterning of hydrogel films soaked in aqueous solution of encapsulated azobenzenes (Fig. 21d and e). Switching was not observed for free azobenzenes in the solid state, supporting the crucial role of the host in enabling photoisomerization.

Similarly, cocrystals of self-assembled SP and γ-cyclodextrin (γCD), SP-COOH@γCD, have been shown to photoisomerize in thin films due to the free volume available in the cavity of γCD. Self-assembly occurs between the carboxylic acid group on the SP molecule and the hydroxy group in γCD, forming a hydrogen bond (Fig. 22a). Hydrogen bonding has shown to be crucial in the formation of 1-dimensional microcrystals in the solid state (Fig. 22b, left) with fluorescence response upon UV irradiation. Furthermore, it was shown that neutralizing the carboxylic acid group on the SP moiety to sodium carboxylate transformed the rod-like microcrystals into a disordered arrangement of clusters (Fig. 22b, right), as observed with scanning electron microscopy [81].

Liu et al. set out to study a DAE guest-host complex in the solid state [82] (Fig. 23). The DAE derivative contains a perfluorinated cyclopentene as well as a diarylammonium functional group. Benzylammonium groups bind to 8-crown ether groups functionalized to $[Ru(bpy)_3]^{2+}$, allowing for the non-covalent interactions between DAE guest moiety and the host. This system shows potential for external optical control of luminescence and Förster resonance energy transfer between host and guest, including demonstrated performance as a novel photoerasable fluorescent inks. The absorbance spectra of the closed DAE isomer overlaps with the emission spectra of the Ru-donor host complex, thus

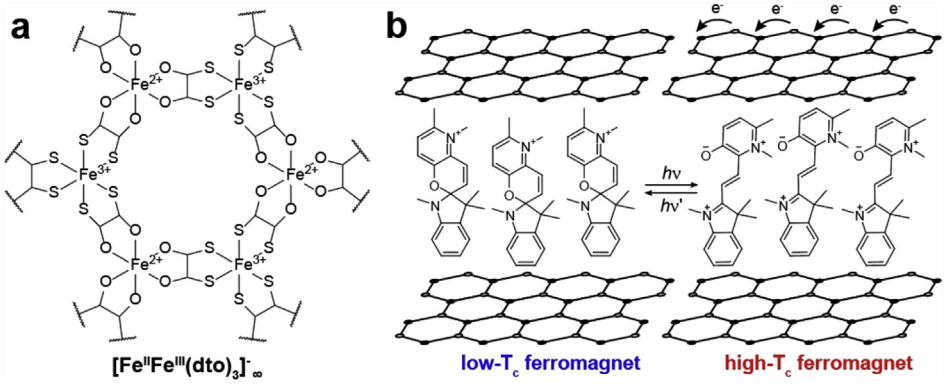

Fig. 17. (a) Representative structure of $[Fe^{II}Fe^{III}(dto)_3]^-_\infty$. (b) Schematic representation of the concerted phenomenon coupled with the charge transfer phase transition in $[Fe^{II}Fe^{III}(dto)_3]^-_\infty$, and the photoisomerization of cationic spiropyrans in $[Fe^{II}Fe^{III}(dto)_3]$. White circles and black circles in the 2D structure represent Fe^{II} and Fe^{III}, respectively. Reproduced and adapted with permission from Ref. [74]. Copyright 2009 American Chemical Society.

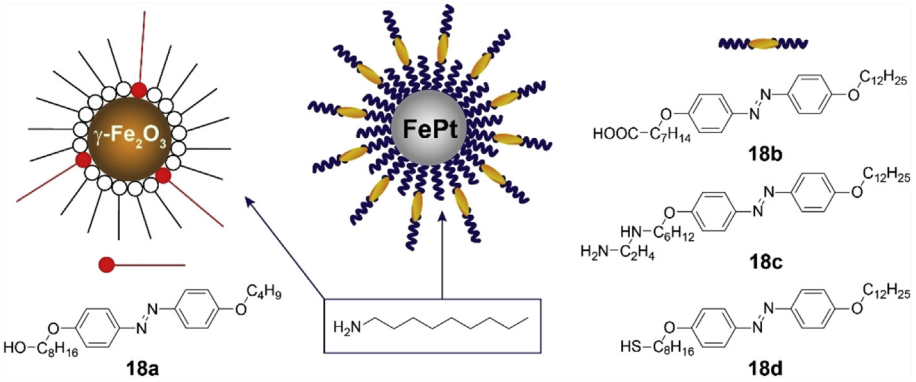

Fig. 18. Structures of γ-Fe_2O_3 (left) and FePt (right) nanoparticles functionalized with azobenzene derivatives **18a** and **18b-d**, respectively. Reproduced and adapted with permission from Ref. [75]. Copyright 2014 Wiley-VCH Verlag GmbH & Co. KGaA. Adapted with permission from Ref. [77]. Copyright 2007 American Chemical Society.

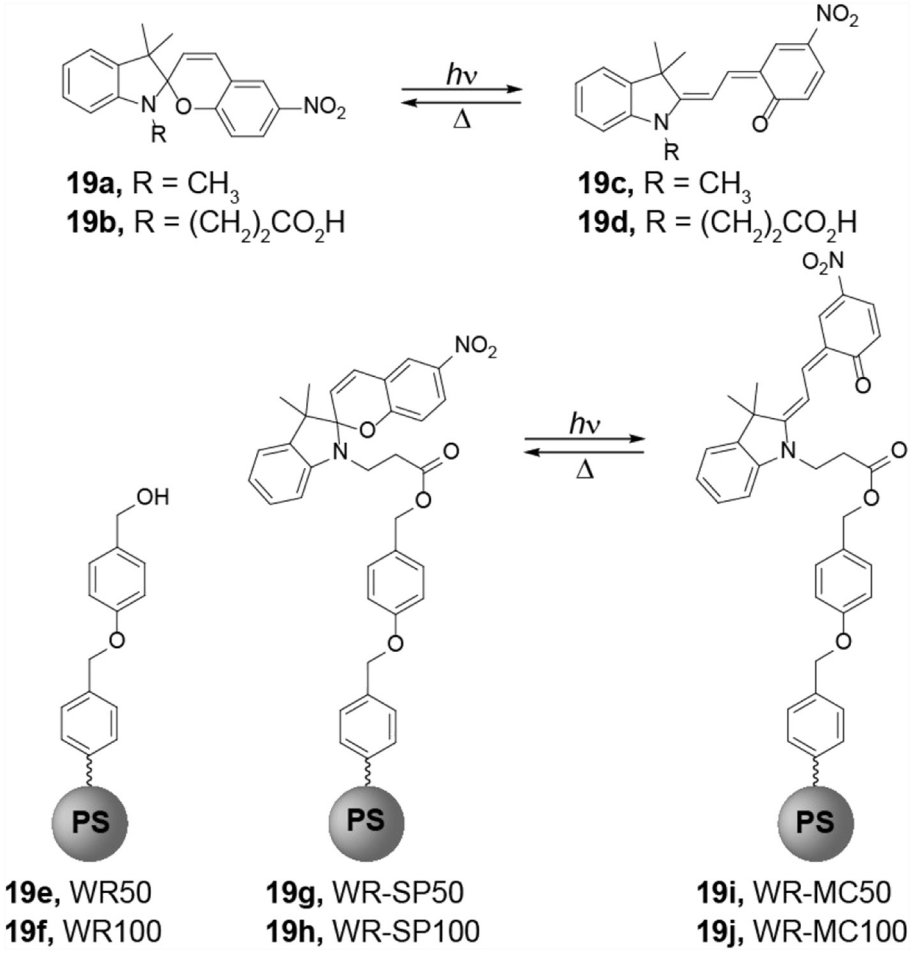

Fig. 19. Structures and photoisomerization of unbound spiropyran (**19a-d**) and spiropyran bound to cross-linked polystyrene Wang resin (WR) (**19g-j**) containing hydroxymethyl reactive sites (**19e, f**). Irradiation was performed with UV light (365 nm) and thermal reversion was performed in the dark at room temperature. WR50 and WR100 represent cross-linked polystyrene WR microparticles of 50 μm and 100 μm, respectively. Reproduced and adapted from Ref. [78] with permission from The Royal Society of Chemistry.

quenching the fluorescence from Ru complex (Fig. 23). Notably, the host-guest complex was able to photoswitch more efficiently in solid state (98%) than in solution (90.6%), granted by efficient transfer of energy from the host molecule to DAE. The rate of photoswitching in solid state (9.6×10^{-3} s^{-1}) was also enhanced compared to that in solution (8.4×10^{-3} s^{-1}). It is proposed that improved photoswitching in the solid state is due to the fixed antiparallel conformation of DAE during photocyclization.

4. Photoswitches on surfaces

Incorporating photoswitches onto surfaces of various materials, one can control optoelectronic properties of such surfaces and generate photoresponsive electronic devices. The interaction between the switches and surfaces can affect the properties of both, and such interaction can be monitored by atomic-resolution imaging techniques [83].

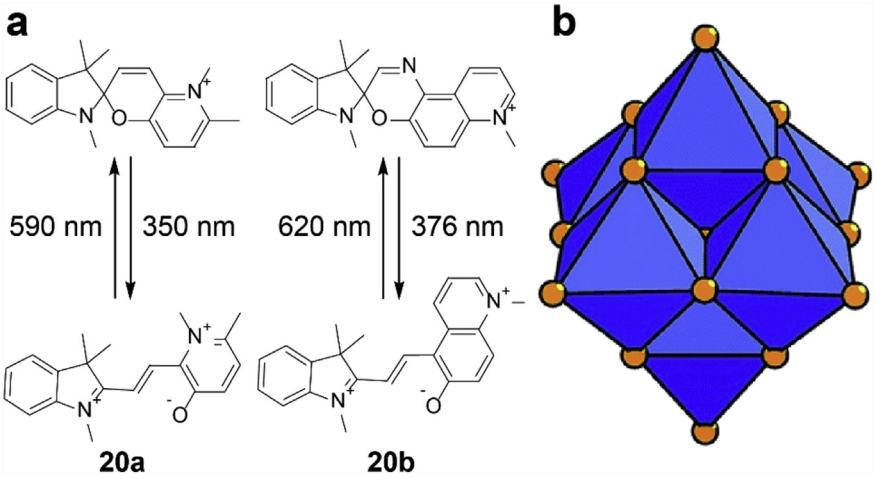

Fig. 20. (a) Photoisomerization of **20a** and **20b**. (b) Polyhedral representation of the POM anion with formula $[M_6O_{19}]^{2-}$ where M = Mo, W (bottom). The gold spheres represent oxygen atoms. Reproduced and adapted from Ref. [79] with permission from The Royal Society of Chemistry. POM, polyoxometalate.

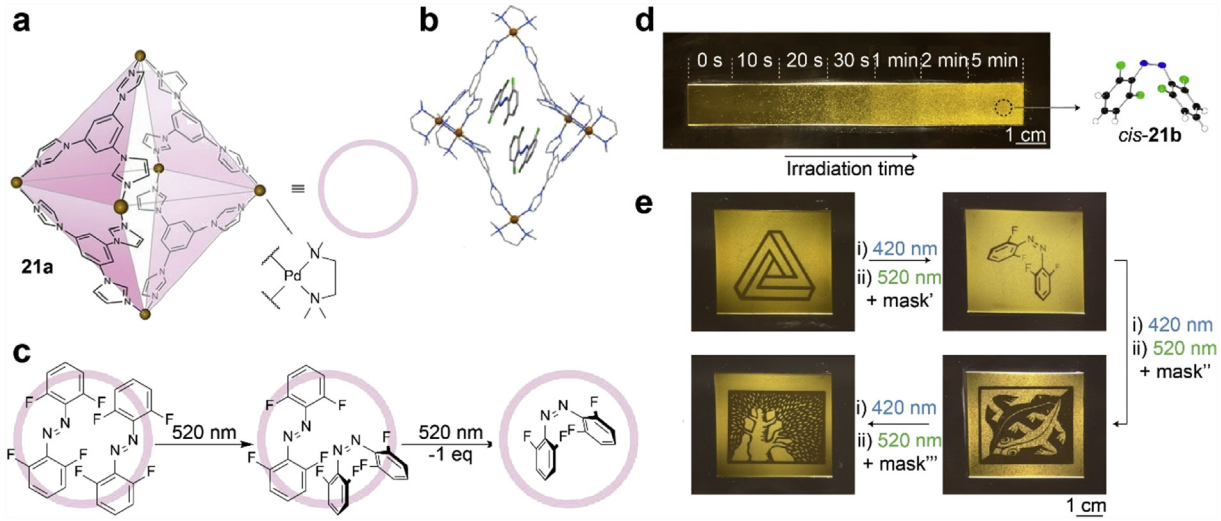

Fig. 21. (a) Structure of polyimidazole-Pd acceptor cage complex **21a** (pink circle). (b) X-ray crystal structure of *trans*-**21b** encapsulated within **21a** (**21b$_2$** ⊂ **21a**). (c) Stepwise mechanism of *trans*-to-*cis* isomerization for **21b$_2$** ⊂ **21a** facilitating the expulsion of one azobenzene derivative from the cage system. (d) Thin piece of agarose gel soaked with an aqueous solution of *trans*-**21b$_2$** ⊂ **21a** irradiated with 520-nm light and corresponding changes over periods of time. (e) Images made consecutively on agarose gel soaked with *trans*-**21b$_2$** ⊂ **21a**. Reproduced and adapted with permission from Ref. [80]. Copyright (2018) National Academy of Sciences.

4.1. Imaging of photoswitching on surfaces

Using annular dark-field scanning transmission electron microscopy, Han et al. were able to directly image the movement of both individual and groups of platinum-decorated azobenzene photoswitches on graphene substrates (Fig. 24a). The heavy platinum atoms serve as markers for distinguishing the photoswitches from the substrate, enabling to track molecular length changes measured between Pt atoms upon photoisomerization. The length change between *trans* (~2.1 nm) and *cis* (~1.4 nm) conformations upon UV irradiation of solid-state photoswitches over graphene was measured at atomic resolution. Moreover, light-activated diffusion of photoswitches was observed, along with the temporary *cis* isomer packing on graphene surface. This study shows promise toward integration of organic photoswitches into 2D materials [83].

Using atomic force microscopy imaging, photoswitching between *cis* and *trans* isomers of AB derivative **24** on a surface of calcite was observed (Fig. 24b–e). Unlike metal surfaces, the insulating surface of calcite kinetically traps the *cis* form upon adsorption, hindering isomerization to the energetically favorable *trans* isomer. Upon *trans-cis-trans* isomerization with alternating UV and visible light, it was revealed that **24** on calcite was reversible and only the *trans* isomer was mobile upon illumination, further supporting that the *cis* isomer is trapped by calcite. In addition, the cross sections of photoisomerization at 455 nm determined on calcite surfaces (~10^{-18} cm^{-2}) were at least two orders of magnitude higher than those observed on metal surfaces (>10^{-20} cm^{-2}) with various wavelengths and comparable to the photoisomerization in solution state (~10^{-19} cm^{-2}), indicating preservation of switching efficiency and photochromic properties on calcite surface [84].

Scanning tunneling microscopy (STM) has been used to image switching of films composed of azobenzene derivatives 4-(phenylazo) benzoic acid (PABA) [85,86] and 4-((1,3,5-trimethyl-1H-pyrazol-4-yl)diazenyl) benzoic acid (PyABA) on highly oriented pyrolytic graphite (Fig. 24f–k). STM images show that films for both derivatives are crystalline and consist of dimers. Upon irradiation of

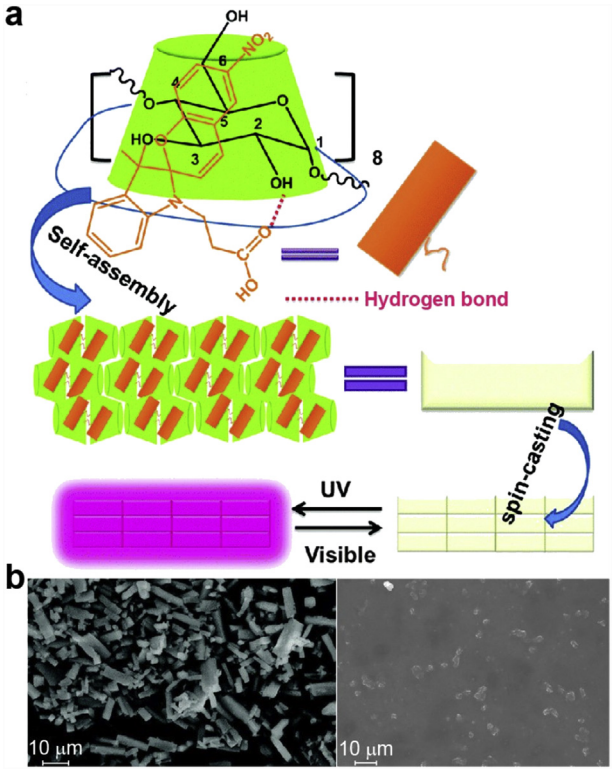

Fig. 22. (a) Scheme illustrating self-assembly of SP-COOH@γCD and fabrication of the solid film. (b) SEM images of SP-COOH@γCD (left) and SP-COOH@γCD after addition of NaOH (right). Reproduced and adapted from Ref. [81] with permission from The Royal Society of Chemistry. SEM, scanning electron microscopy.

UV light (370 nm), it was observed that for both PABA and PyABA, the unsubstituted ring switches away from the surface plane. The carboxyl group provides intermolecular interactions between neighboring molecules that physically keep the *cis* structures on the surface. It is interesting to note that switching only occurs for alternating rows of dimers in PABA, whereas switching is observed for all molecules in PyABA film [86].

4.2. Nanoscale devices incorporating photoswitches on surfaces

Azobenzenes have been physisorbed on semiconductors to develop van der Waals heterostructures as a means to realize nanoscale transistors. Using photoswitches, the properties of 2D semiconducting materials can be controlled by light irradiation; however, the persistent photoconductivity effect (PPC), a common occurrence on the interface of 2D semiconducting materials, hinders fast response. By employing a trap-free polymer dielectric as a support for the AZO/MoS_2 hybrid system, the PPC effect was suppressed. Raman spectroscopy, photoluminescence spectroscopy, and I–V measurements revealed that photoswitching of azobenzene molecules adsorbed on the n-type MoS_2 surface was reversible, with the *trans* form inducing n-type doping compared to the non-functionalized MoS_2 and the *cis* form inducing p-type doping (Fig. 25a). Azobenzene molecules were also adsorbed onto black phosphorous to develop p-n diodes that were controlled by photoswitching (Fig. 25b). *Cis-trans* isomerization of adsorbed azobenzene molecules under light irradiation demonstrates control over the dipole moment and carrier concentration within hybrid structures [87].

DHA/VHF systems have also been applied to solid-state molecular junctions as self-assembled monolayers (SAMs) on gold and ITO surfaces. The former was accomplished using an acetyl-protected thiolate anchoring group on the *meta* position of the DHA phenylene unit to reduce surface quenching (Fig. 25c). In addition, application of reduced graphene oxide (rGO) films as a soft top-contact enabled *in situ* photoswitching along with charge transport measurements. It should be noted that DHA-based SAMs showed higher conductivity than VHF-based SAMs, and switching between the two forms was made possible by alternating between

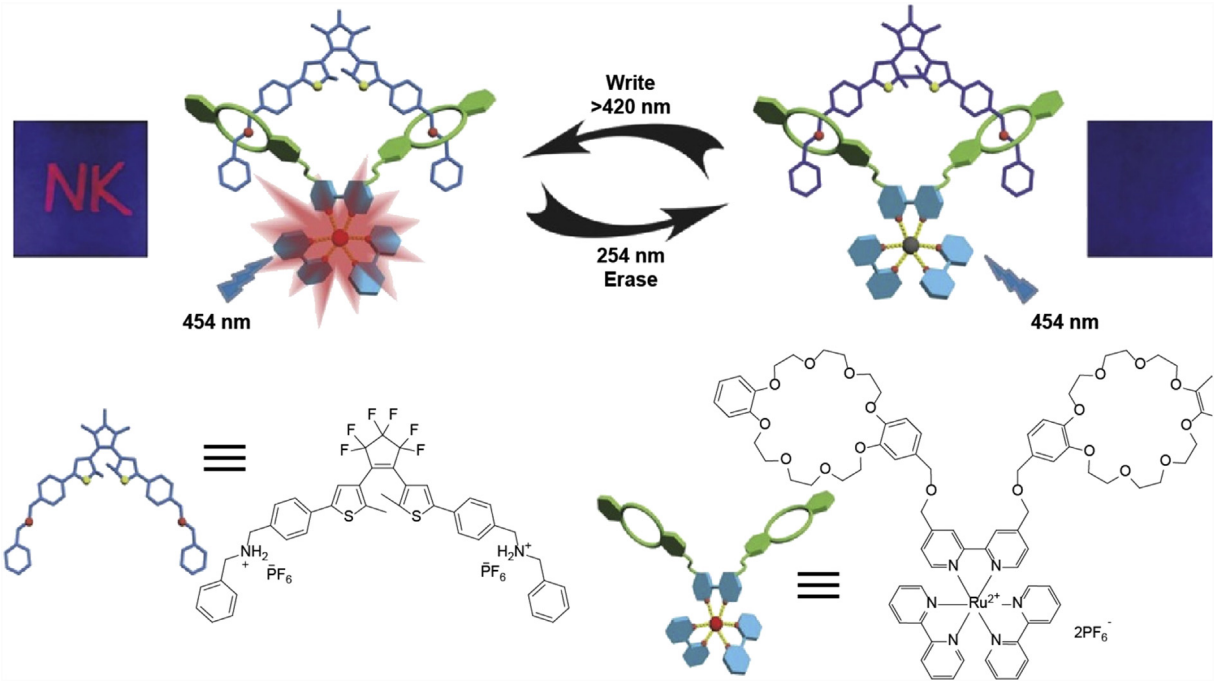

Fig. 23. Supramolecular interaction of DAE guest molecule and Ru complex host molecule demonstrating an efficient patterning. Irradiation of 454-nm light results in red light emission from host complex. Reproduced and adapted with permission from Ref. [82]. Copyright 2016 Wiley-VCH Verlag GmbH & Co. KGaA. DAE, diarylethenes.

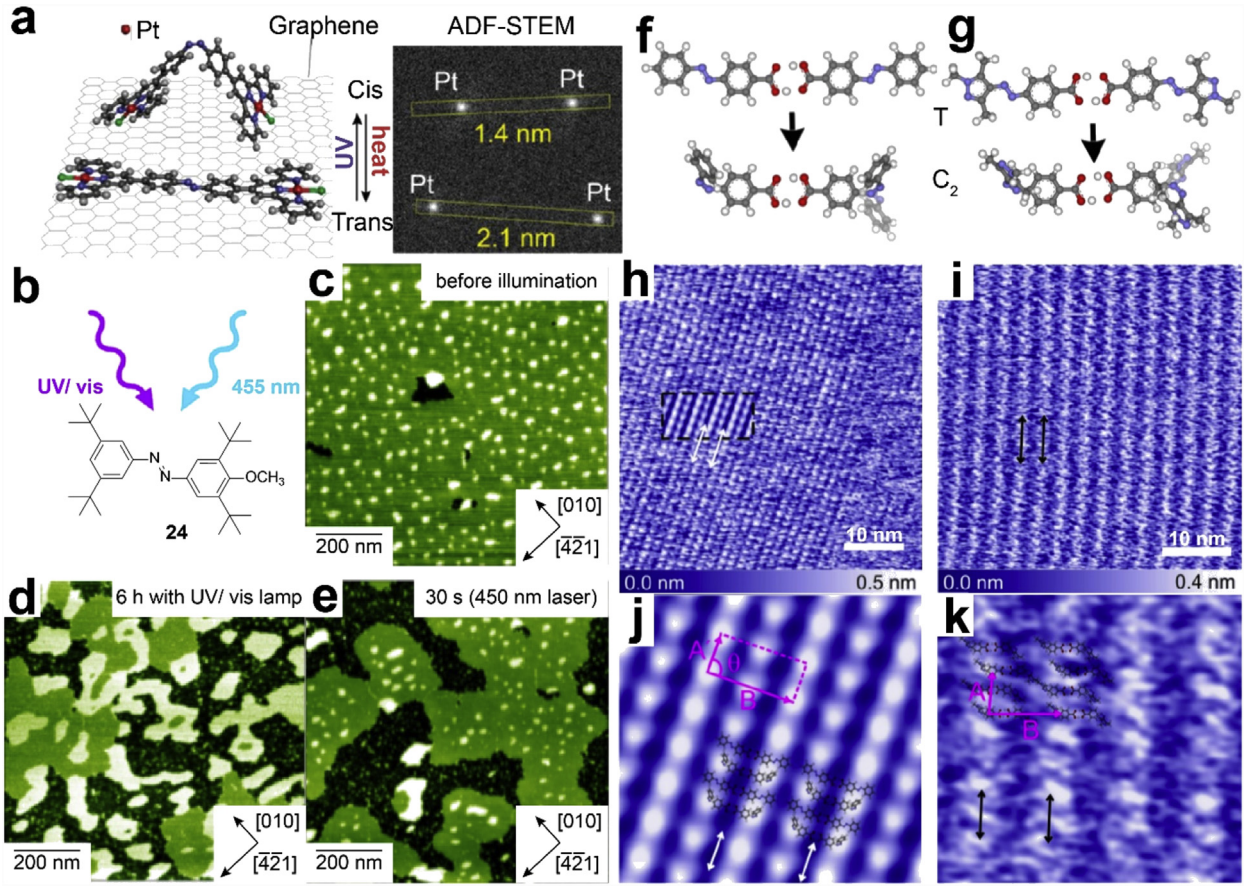

Fig. 24. (a) Atomic model of *cis* and *trans* isomers of Pt(II)-azobenzene on a graphene monolayer substrate and multislice high-angle ADF-STEM image simulation showing the high contrast from platinum atoms of Pt(II)-azobenzene isomers. Reproduced and adapted with permission from Ref. [83]. Copyright 2019 American Chemical Society. (b) Azobenzene derivative **24** and (c–e) AFM image of calcite surface with *trans* (green) and *cis* (white) forms of AFM images (all 1 × 1 μm^2 in size). AFM images obtained (c) directly after sample preparation and after illumination with a broadband UV–vis lamp for (d) 6 h, after illumination with a 450-nm laser for (e) 30 s. Reproduced and adapted with permission from Ref. [84]. Copyright 2018 American Chemical Society. (f–g) Schematics showing *trans–trans* (**T**) and *cis–cis* (**C$_2$**) dimers of (f) PABA and (g) pyABA. The shaded part of **C$_2$** dimer shows other possible configuration with respect to surface plane after switching. (h–i) Typical constant current STM topograph of adlayers of (h) PABA (0.88 V, 96 pA) and (i) PyABA (0.87 V, 90 pA) on HOPG after illumination of UV light (370 nm). (j–k) Averaged STM image overlaid with scaled *cis* and *trans* dimers. Reproduced and adapted with permission from Ref. [86]. Copyright 2018 American Chemical Society. ADF-STEM, annular dark-field scanning transmission electron microscopy; AFM, atomic force microscopy; PABA, 4-(phenylazo) benzoic acid; PyABA, 4-((1,3,5-trimethyl-1H-pyrazol-4-yl)diazenyl) benzoic acid; STM, scanning tunneling microscopy; HOPG, highly oriented pyrolytic graphite.

UV irradiation and thermal annealing at 70 °C. The reason for differences in conductivity arise from the differences in surface morphology. DHA has reduced conformational flexibility compared to VHF; therefore, photoswitching moieties are located close enough to the top contact to contribute to electron transport [88].

5. Summary and outlook

A variety of photoswitches and their isomerization dynamics in solid state have been reviewed along with the effective strategies for enhancing the switching probabilities. Because photoisomerization often involves the rotation of molecular structures, the compact environment in solid state and the strong intermolecular interactions significantly limit the structural change. The covalent functionalization of pristine photoswitching cores with bulky substituents or amorphous polymer backbones has been demonstrated to render structural voids within films or powders, which allows for the less hindered isomerization. Various templates including MOFs, carbon nanomaterials, nanoparticles, and nanocages were also introduced as a means to grant rotational freedom to photoswitches within solid platforms. The switches deposited on surface of 2D materials, metals, and insulators were monitored by microscopy techniques to gauge their nanoscale movement and interaction with the underlying substrates. The integration of organic photoswitches with inorganic surfaces presents an opportunity to construct next-generation low-power electronic devices such as light-activated transistors or photodetectors which reversibly operate at the speed of photoswitching. The conformational change in switches will correlate to the electrical output of the ultra-thin devices composed of atomically thin 2D materials and self-assembly monolayer of organic photoswitches. Another exciting field of opto-spintronics also takes advantage of photoswitching molecules to control quantum systems and thin-film devices.

Thus, it is envisioned that facile solid-state switching of organic molecules, particularly at the interface with other functional materials, will contribute to the development of new light-controlled materials, switchable devices, and photon energy storage materials. One of the intrinsic challenges in achieving such applications is the limited light penetration or absorption through thick films or bulk materials. The photoisomers often exhibit overlapping light absorption spectra, preventing 100% saturated photostationary state of either isomeric form, even in dilute solution state. In the condensed phase, due to the increased concentration of photoisomers, the light penetration is further limited to micron scale [89], in case of azobenzene materials. The depth of light penetration

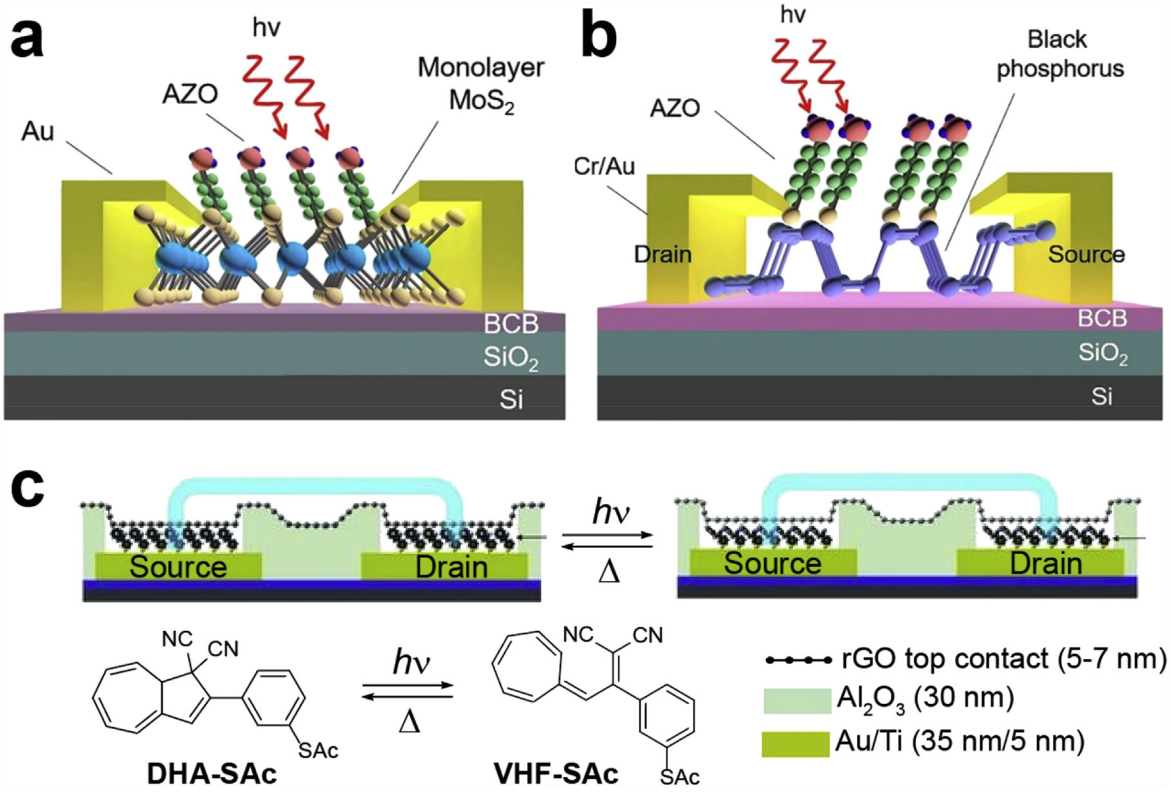

Fig. 25. Scheme of the hybrid field-effect transistor structure with the physisorption of azo molecules on (a) MoS_2 and (b) black phosphorous surface. Reproduced and adapted with permission from Ref. [87]. Copyright 2019 American Chemical Society. (c) Cross section of molecular junction with SAM composed of thermo-optical switch DHA-SAc/VHF-SAc. Reproduced and adapted with permission from Ref. [88]. Copyright 2013 Wiley-VCH Verlag GmbH & Co. KGaA. DHA, 1,8a-dihydroazulene-1,1-dicarbonitrile; SAM, self-assembled monolayers; VHF, vinylheptafulvene; SAc, thioacetate; ITO, indium tin oxide.

depends on the spectral separation between the isomers of each compound, which can be improved by the covalent functionalization methods. Some efforts have been dedicated on separating n−π* bands of *trans* and *cis* isomers of azobenzene by functionalizing *ortho* positions of core structures with methoxy [90], fluorine [91], and other halide groups [92]. Bridging the *ortho* positions with ethane group [93] was also reported to increase the spectral separation of each isomer. Based on the current development, it is expected that selective excitation of one isomer over the other will be accomplished by light irradiation, and the generated photoisomer will not hinder the light absorption of the original isomers even in condensed phase. The strategies to shift light absorption spectra and to induce unhindered structural change can be combined to achieve the solid-state bulk materials with high photoswitching capabilities.

Other challenges such as low quantum yields of switching for some photoisomers and low thermal stability of metastable isomers will be also addressed by the functionalization of known photoswitching cores or the development of new switch structures. Heteroaryl azobenzenes [94–99], for example, have been recently developed to significantly increase the half-life of metastable *cis* isomers through the engineering of metastable structures. For the practical solid-state applications, the switching kinetics and efficiency, wavelengths of light for activation, and stability of solid will need to be considered, and the solid-state characterization techniques such as variable-temperature film measurements, *in situ* heating/light irradiation microscopy, and *in situ* irradiation calorimetry will be employed to provide real-time observation of solid-state property changes.

Declaration of competing interest

The authors declare that they have no known competing financial interests or personal relationships that could have appeared to influence the work reported in this paper.

Acknowledgments

A.G. was supported by Myron Rosenblum Endowed Fellowship from Brandeis University.

References

[1] C.-L. Sun, C. Wang, R. Boulatov, Applications of photoswitches in the storage of solar energy, ChemPhotoChem 3 (2019) 268–283.
[2] D. Zhao, Y. Qiu, W. Cheng, S. Bi, H. Wang, Q. Wang, Y. Liao, H. Peng, X. Xie, Precisely tuning helical twisting power via photoisomerization kinetics of dopants in chiral nematic liquid crystals, Langmuir 34 (2018) 700–708.
[3] H. Yang, M. Li, C. Li, Q. Luo, M.-Q. Zhu, H. Tian, W.-H. Zhu, Unraveling dual aggregation-induced emission behavior in steric-hindrance photochromic system for super resolution imaging, Angew. Chem. Int. Ed. (2019), https://doi.org/10.1002/anie.201909830.
[4] Z. Li, C. He, Y. Li, Y. Wang, C. Wei, J. Yin, S.H. Liu, Construction and optical properties of dithienylethene-based photoswitchable [n] rotaxane (n= 2, 3), Dyes Pigments 148 (2018) 130–136.
[5] Y. Lin, H.R. Hansen, W.J. Brittain, S.L. Craig, Strain-dependent kinetics in the cis-to-trans isomerization of azobenzene in bulk elastomers, J. Phys. Chem. B 123 (2019) 8492–8498.
[6] R.H. Zha, G. Vantomme, J.A. Berrocal, R. Gosens, B. de Waal, S. Meskers, E.W. Meijer, Photoswitchable nanomaterials based on hierarchically organized siloxane oligomers, Adv. Funct. Mater. 28 (2017) 1703952.
[7] L. Zou, M.J. Webber, Reversible hydrogel dynamics by physical-chemical crosslink photoswitching using a supramolecular macrocycle template, Chem. Commun. 55 (2019) 9931–9934.

[8] A. Ryabchun, Q. Li, F. Lancia, I. Aprahamian, N. Katsonis, Shape-persistent actuators from hydrazone photoswitches, J. Am. Chem. Soc. 141 (2019) 1196–1200.

[9] G.G.D. Han, S.S. Park, Y. Liu, D. Zhitomirsky, E. Cho, M. Dincă, J.C. Grossman, Photon energy storage materials with high energy densities based on diacetylene-azobenzene derivatives, J. Mater. Chem. A 4 (2016) 16157–16165.

[10] F. Waidhas, M. Jevric, L. Fromm, M. Bertram, A. Görling, K. Moth-Poulsen, O. Brummel, J. Libuda, Electrochemically controlled energy storage in a norbornadiene-based solar fuel with 99% reversibility, Nano Energy 63 (2019) 103872.

[11] H. Chen, Y. Zhao, Applications of Light-responsive systems for cancer theranostics, ACS Appl. Mater. Interfaces 10 (2018) 21021–21034.

[12] M. Arczyński, J. Stanek, B. Sieklucka, K.R. Dunbar, D. Pinkowicz, Site-selective photoswitching of two distinct magnetic chromophores in a propeller-like molecule to achieve four different magnetic states, J. Am. Chem. Soc. 141 (2019) 19067–19077.

[13] M.M. Paquette, D. Plaul, A. Kurimoto, B.O. Patrick, N.L. Frank, Opto-spintronics: photoisomerization-induced spin state switching at 300 K in photochrome cobalt-dioxolene thin films, J. Am. Chem. Soc. 140 (2018) 14990–15000.

[14] Z. Ming, X. Hua, Y. Xue, Q. Lin, C. Bao, L. Zhu, Visible light controls cell adhesion on a photoswitchable biointerface, Colloids Surf. B: Biointerfaces 169 (2018) 41–48.

[15] D.E. Williams, C.R. Martin, E.A. Dolgopolova, A. Swifton, D.C. Godfrey, O.A. Ejegbavwo, P.J. Pellechia, M.D. Smith, N.B. Shustova, Flipping the switch: fast photoisomerization in a confined environment, J. Am. Chem. Soc. 140 (2018) 7611–7622.

[16] X. Xiao, J. Hu, X. Wang, L. Huang, Y. Chen, W. Wang, J. Li, Y. Zhang, A dual-functional supramolecular hydrogel based on a spiropyran-galactose conjugate for target-mediated and light-controlled delivery of microRNA into cells, Chem. Commun. 52 (2016) 12517–12520.

[17] X. Fang, H. Zhang, Y. Chen, Y. Lin, Y. Xu, W. Weng, Biomimetic modular polymer with tough and stress sensing properties, Macromolecules 46 (2013) 6566–6574.

[18] H. Koshima, N. Ojima, Photomechanical bending of 4-aminoazobenzene crystals, Dyes Pigments 92 (2012) 798–801.

[19] R. Navrátil, S. Wiedbrauk, J. Jasik, H. Dube, J. Roithová, Transforming hemithioindigo from a two-way to a one-way molecular photoswitch by isolation in the gas phase, Phys. Chem. Chem. Phys. 20 (2018) 6868–6876.

[20] C.Y. Huang, A. Bonasera, L. Hristov, Y. Garmshausen, B.M. Schmidt, D. Jacquemin, S. Hecht, *N,N'*-disubstituted indigos as readily available red-light photoswitches with tunable thermal half-lives, J. Am. Chem. Soc. 139 (2017) 15205–15211.

[21] A. Mostad, C. Romming, A refinement of the crystal structure of cis-azobenzene, Acta Chem. Scand. 25 (1971) 3561–3568.

[22] D. Zhitomirsky, E. Cho, J.C. Grossman, Solid-state solar thermal fuels for heat release applications, Adv. Energy Mater. 6 (2016) 1502006.

[23] T.J. Kucharski, N. Ferralis, A.M. Kolpak, J.O. Zheng, D.G. Nocera, J.C. Grossman, Templated assembly of photoswitches significantly increases the energy-storage capacity of solar thermal fuels, Nat. Chem. 6 (2014) 441.

[24] E.N. Cho, D. Zhitomirsky, G.G.D. Han, Y. Liu, J.C. Grossman, Molecularly engineered azobenzene derivatives for high energy density solid-state solar thermal fuels, ACS Appl. Mater. Interfaces 9 (2017) 8679–8687.

[25] C. Probst, C. Meichner, K. Kreger, L. Kador, C. Neuber, H.W. Schmidt, Athermal azobenzene-based nanoimprint lithography, Adv. Mater. 28 (2016) 2624–2628.

[26] U. Bhattacharjee, D. Freppon, L. Men, J. Vela, E.A. Smith, J.W. Petrich, The photoinduced trans-to-cis phase transition of polycrystalline azobenzene at low irradiances occurs in the solid state, Euro. J. Chem. Phys. Chem. 18 (2017) 2526–2532.

[27] S.M. Landge, I. Aprahamian, A pH activated configurational rotary switch: controlling the E/Z isomerization in hydrazones, J. Am. Chem. Soc. 131 (2009) 18269–18271.

[28] S.M. Landge, E. Tkatchouk, D. Benítez, D.A. Lanfranchi, M. Elhabiri, W.A. Goddard III, I. Aprahamian, Isomerization mechanism in hydrazone-based rotary switches: lateral shift, rotation, or tautomerization? J. Am. Chem. Soc. 133 (2011) 9812–9823.

[29] X. Su, M. Lõkov, A. Kütt, I. Leito, I. Aprahamian, Unusual *para*-substituent effects on the intramolecular hydrogen-bond in hydrazine-based switches, Chem. Commun. 28 (2012) 10490–10492.

[30] Y. Shigeo, T. Takashi, S. Takahiro, S. Masako, K. Yuji, I. Kunihiro, α-Hydrazono-β-keto esters as command molecules, Chem. Lett. 21 (1992) 543–546.

[31] I. Aprahamian, Hydrazone switches and things in between, Chem. Commun. 53 (2017) 6674–6684.

[32] C. Petermayer, H. Dube, Indigoid photoswitches: visible light responsive molecular tools, Acc. Chem. Res. 51 (2018) 1153–1163.

[33] S. Kobatake, T. Yamada, K. Uchida, N. Kato, M. Irie, Photochromism of 1,2-bis(2,5-dimethyl-3-thienyl)perfluorocyclopentene in a single crystalline phase, J. Am. Chem. Soc. 121 (1999) 2380–2386.

[34] M. Irie, T. Fukaminato, K. Matsuda, S. Kobatake, Photochromism of diarylethene molecules and crystals: memories, switches, and actuators, Chem. Rev. 114 (2014) 12174–12277.

[35] T. Fukaminato, T. Doi, N. Tamaoki, K. Okuno, Y. Ishibashi, H. Miyasaka, M. Irie, Single-molecule fluorescence photoswitching of a diarylethene–perylenebisimide dyad: non-destructive fluorescence readout, J. Am. Chem. Soc. 133 (2011) 4984–4990.

[36] U. Bauer, L. Fromm, C. Weiß, P. Bachmann, F. Späth, F. Düll, J. Steinhauer, W. Hieringer, A. Görling, A. Hirsch, H.-P. Steinrück, C. Papp, Controlled catalytic energy release of the norbornadiene/quadricyclane molecular solar thermal energy storage system on Ni(111), J. Phys. Chem. C 123 (2019) 7654–7664.

[37] I. Nishimura, A. Kameyama, T. Sakurai, T. Nishikubo, Synthesis of polyesters carrying norbornadiene (NBD) moieties by the ring-opening copolymerization of glycidyl esters containing NBD moieties with carboxylic anhydrides and their photochemical reactions, Macromolecules 29 (1996) 3818–3825.

[38] A.U. Petersen, A.I. Hofmann, M. Fillols, M. Mansø, M. Jevric, Z. Wang, C.J. Sumby, C. Müller, K. Moth Poulsen, Solar energy storage by molecular norbornadiene–quadricyclane photoswitches: polymer film device, Adv. Sci. 6 (2019) 1900367.

[39] S.L. Broman, M.B. Nielsen, Dihydroazulene: from controlling photochromism to molecular electronics devices, Phys. Chem. Chem. Phys. 16 (2014) 21172–21182.

[40] B.N. Frandsen, A.B. Skov, M. Cacciarini, M. Brøndsted Nielsen, H.G. Kjaergaard, Computational and experimental evidence of two competing thermal electrocyclization pathways for vinylheptafulvene, Chem. Asian J. 14 (2019) 1111–1116.

[41] C.B. Aakeröy, E.P. Hurley, J. Desper, M. Natali, A. Douglawi, S. Giordani, The balance between closed and open forms of spiropyrans in the solid state, CrystEngComm 12 (2010) 1027–1033.

[42] S.A. Krysanov, M.V. Alfimov, Ultrafast formation of transients in spiropyran photochromism, Chem. Phys. Lett. 91 (1982) 77–80.

[43] J. Harada, Y. Kawazoe, K. Ogawa, Photochromism of spiropyrans and spirooxazines in the solid state: low temperature enhances photocoloration, Chem. Commun. 46 (2010) 2593–2595.

[44] D.A. Parthenopoulos, P.M. Rentzepis, Three-dimensional optical storage memory, Science 245 (1989) 843–845.

[45] C. Özçoban, T. Halbritter, S. Steinwand, L.M. Herzig, J. Kohl-Landgraf, N. Askari, F. Groher, B. Fürtig, C. Richter, H. Schwalbe, B. Suess, J. Wachtveitl, A. Heckel, Water-soluble py-BIPS spiropyrans as photoswitches for biological applications, Org. Lett. 17 (2015) 1517–1520.

[46] C. Brieke, A. Heckel, Spiropyran photoswitches in the context of DNA: synthesis and photochromic properties, Chem. Eur. J. 19 (2013) 15726–15734.

[47] R. Klajn, Spiropyran-based dynamic materials, Chem. Soc. Rev. 43 (2014) 148–184.

[48] K. Arai, Y. Kobayashi, J. Abe, Rational molecular designs for drastic acceleration of the color-fading speed of photochromic naphthopyrans, Chem. Commun. 51 (2015) 3057–3060.

[49] J. Harada, K. Ueki, M. Anada, Y. Kawazoe, K. Ogawa, Solid-state photochromism of chromenes: enhanced photocoloration and observation of unstable colored species at low temperatures, Chem. Eur J. 17 (2011) 14111–14119.

[50] A. Migani, P.L. Gentili, F. Negri, M. Olivucci, A. Romani, G. Favaro, R.S. Becker, The ring-opening reaction of chromenes: A photochemical mode-dependent transformation, J. Phys. Chem. A 109 (2005) 8684–8692.

[51] A. Gerwien, M. Schildhauer, S. Thumser, P. Mayer, H. Dube, Direct evidence for hula twist and single-bond rotation photoproducts, Nat. Commun. 9 (2018) 2510.

[52] I. Liepuoniute, P. Commins, D.P. Karothu, S. Schramm, H. Hara, P. Naumov, Reversible multicolor photochromism of dihydroazulene crystals, Chem. Eur J. 25 (2019) 373–378. K.

[53] V.M. Breslin, N.A. Barbour, D.K. Dang, S.A. Lopez, M.A. Garcia-Garibay, Nanosecond laser flash photolysis of a 6-nitroindolinospiropyran in solution and in nanocrystalline suspension under single excitation conditions, Photochem. Photobiol. Sci. 17 (2018) 741–749.

[54] S. Bénard, P. Yu, New spiropyrans showing crystalline-state photochromism, Adv. Mater. 12 (2000) 48–50.

[55] M.A. Gerkman, S. Yuan, P. Duan, J. Taufan, K. Schmidt-Rohr, G.G.D. Han, Phase transition of spiropyrans: impact of isomerization dynamics at high temperatures, Chem. Commun. 55 (2019) 5813–5816.

[56] S. Kambe Kasatani, M. Irie, Photochromic reaction and fluorescence of dithienylethenes in the solid state, J. Photochem. Photobiol. A: Chem. 122 (1999) 11–15.

[57] M. Baroncini, S. d'Agostino, G. Bergamini, P. Ceroni, A. Comotti, P. Sozzani, I. Bassanetti, F. Grepioni, T.M. Hernandez, S. Silvi, M. Venturi, A. Credi, Photoinduced reversible switching of porosity in molecular crystals based on star-shaped azobenzene tetramers, Nat. Chem. 7 (2015) 634–640.

[58] A. Sekine, H. Yamagiwa, H. Uekusa, Novel solid-state photochromic reaction of azobenzene derivative controlled by appended photoreactive group, Chem. Lett. 41 (2012) 795–797.

[59] O.S. Bushuyev, A. Tomberg, T. Friščić, C.J. Barrett, Shaping crystals with light: crystal-to-crystal isomerization and photomechanical effect in fluorinated azobenzenes, J. Am. Chem. Soc. 135 (2013) 12556–12559.

[60] O.S. Bushuyev, T.C. Corkery, C.J. Barrett, T. Friščić, Photo-mechanical azobenzene cocrystals and in situ X-ray diffraction monitoring of their optically-induced crystal-to-crystal isomerisation, Chem. Sci. 8 (2014) 3158–3164.

[61] D.J.V. Dijken, Petr Kovaříček, S.P. Ihrig, S. Hecht, Acylhydrazones as widely tunable photoswitches, J. Am. Chem. Soc. 137 (2015) 14982–14991.

[62] B. Shao, M. Baroncini, H. Qian, L. Bussotti, M. Di Donato, A. Credi, I. Aprahamian, Solution and solid-state emission toggling of a photochromic hydrazone, J. Am. Chem. Soc. 140 (2018) 12323–12327.
[63] B. Shao, H. Qian, Q. Li, I. Aprahamian, Structure property analysis of the solution and solid-state properties of bistable photochromic hydrazones, J. Am. Chem. Soc. 141 (2019) 8364–8371.
[64] Z. Wu, K. Pan, S. Mo, B. Wang, X. Zhao, M. Yin, Tetraphenylethene-induced free volumes for the isomerization of spiropyran toward multifunctional materials in the solid state, ACS Appl. Mater. Interfaces 10 (2018) 30879–30886.
[65] Q. Qi, C. Li, X. Liu, S. Jiang, Z. Xu, R. Lee, M. Zhu, B. Xu, W. Tian, Solid-state photoinduced luminescence switch for advanced anticounterfeiting and super-resolution imaging applications, J. Am. Chem. Soc. 139 (2017) 16036–16039.
[66] P. Weis, D. Wang, S. Wu, Visible-light-responsive azopolymers with inhibited π–π stacking enable fully reversible photopatterning, Macromolecules 49 (2016) 6368–6373.
[67] H. Zhou, C. Xue, P. Weis, Y. Suzuki, S. Huang, K. Koynov, G.K. Auernhammer, R. Berger, H.J. Butt, S. Wu, Photoswitching of glass transition temperatures of azobenzene-containing polymers induces reversible solid-to-liquid transitions, Nat. Chem. 9 (2017) 145–151.
[68] Q. Liu, K. Jiang, Y. Wen, J. Wang, J. Luo, Y. Song, High-performance optoelectrical dual-mode memory based on spiropyran-containing polyimide, Appl. Phys. Lett. 97 (2010) 253304.
[69] A. Oueslati, I. Abdelhedi, R. Mercier, E. Drockenmuller, H.B. Romdhane, Photoresponsive polyamides containing pentamethylated norbornadiene moieties: synthesis and photochemical properties under sunlight irradiation, J. Polym. Sci., Polym. Chem. 51 (2013) 4650–4656.
[70] Y. Jiang, J. Huang, W. Feng, X. Zhao, T. Wang, C. Li, W. Luo, Molecular regulation of nano-structured solid-state AZO-SWCNTs assembly film for the high-energy and short-term solar thermal storage, Sol. Energy Mater. Sol. Cells 193 (2019) 198–205.
[71] Q. Yan, Y. Zhang, Y. Dang, Y. Feng, W. Feng, Solid-state high-power photo heat output of 4-((3,5-dimethoxyaniline)-diazenyl)-2-imidazole/graphene film for thermally controllable dual data encoding/reading, Energy Storage Mater. (2019), https://doi.org/10.1016/j.ensm.2019.06.005.
[72] T. Yamaguchi, A. Maity, V. Polshettiwar, M. Ogawa, Negative photochromism based on molecular diffusion between hydrophilic and hydrophobic particles in the solid state, Inorg. Chem. 57 (2018) 3671–3674.
[73] E.A. Dolgopolova, A.M. Rice, C.R. Martin, N.B. Shustova, Photochemistry and photophysics of MOFs: steps towards MOF-based sensing enhancements, Chem. Soc. Rev. 47 (2018) 4710–4728.
[74] N. Kida, M. Hikita, I. Kashima, M. Okubo, M. Itoi, M. Enomoto, K. Kato, M. Takata, N. Kojima, Control of charge transfer phase transition and ferromagnetism by photoisomerization of spiropyran for an organic–inorganic hybrid system, (SP)[$Fe^{II}Fe^{III}$(dto)$_3$] (SP = spiropyran, dto = $C_2O_2S_2$), J. Am. Chem. Soc. 131 (2009) 212–220.
[75] R. Mikami, M. Taguchi, K. Yamada, K. Suzuki, O. Sato, Y. Einaga, Reversible photo-switching of the magnetization of iron oxide nanoparticles at room temperature, Angew. Chem. Int. Ed. 43 (2004) 6135–6139.
[76] M. Taguchi, G. Li, Z. Gu, O. Sato, Y. Einaga, Magnetic vesicles of amphiphilic spiropyran containing iron oxide particles on a solid state substrate, Chem. Mater. 15 (2003) 4756–4760.
[77] M. Suda, M. Nakagawa, T. Iyoda, Y. Einaga, Reversible photoswitching of ferromagnetic FePt nanoparticles at room temperature, J. Am. Chem. Soc. 129 (2007) 5538–5543.
[78] J. Whelan, D. Abdallah, J. Wojtyk, E. Buncel, Micro-environmental fine-tuning of electronic and kinetic properties of photochromic dyes, J. Mater. Chem. 20 (2010) 5727–5735.
[79] C. Menet, H. Serier-Brault, O. Oms, A. Dolbecq, J. Marrot, A. Saad, P. Mialane, S. Jobic, P. Deniard, R. Dessapt, Influence of electronic vs. steric factors on the solid-state photochromic performances of new polyoxometalate/spirooxazine and spiropyran hybrid materials, RSC Adv. 5 (2015) 79635–79643.
[80] D. Samanta, J. Gemen, Z. Chu, Y. Diskin-Posner, L.J.W. Shimon, R. Klajn, Reversible photoswitching of encapsulated azobenzenes in water, Proc. Natl. Acad. Sci. U.S.A. 115 (2018) 9379–9384.
[81] B. Lv, Z. Wu, C. Ji, W. Yang, D. Yan, M. Yin, Spiropyran-induced one-dimensional cyclodextrin microcrystals with light-driven fluorescence change, J. Mater. Chem. C 3 (2015) 8519–8525.
[82] H. Wu, Y. Chen, Y. Liu, Reversibly Photoswitchable supramolecular assembly and its application as a photoerasable fluorescent ink, Adv. Mater. 29 (2017) 1605271.
[83] M.A. Gerkman, S. Sinha, J.H. Warner, G.G.D. Han, Direct imaging of photoswitching molecular conformations using individual metal atom markers, ACS Nano 13 (2019) 87–96.
[84] S. Jaekel, A. Richter, R. Lindner, R. Bechstein, C. Nacci, S. Hecht, A. Kühnle, L. Grill, Reversible and efficient light-induced molecular switching on an insulator surface, ACS Nano 12 (2018) 1821–1828.
[85] K. Yadav, T. Halbritter, A. Heckel, T.G. Gopakumar, Controlling self-assembly of switchable azobenzene derivatives on highly oriented pyrolytic graphite at ambient conditions, J. Phys. Chem. C 122 (2018) 15330–15337.
[86] K. Yadav, S. Mahapatra, T. Halbritter, A. Heckel, T.G. Gopakumar, Low-threshold reversible electron-induced and selective photoinduced switching of azobenzene derivatives under ambient conditions, J. Phys. Chem. Lett. 9 (2018) 6326–6333.
[87] Y. Zhao, S. Bertolazzi, P. Samorì, A universal approach toward light-responsive two-dimensional electronics: chemically tailored hybrid van der Waals heterostructures, ACS Nano 13 (2019) 4814–4825.
[88] T. Li, M. Jevric, J.R. Hauptmann, R. Hviid, Z. Wei, R. Wang, N.E. Reeler, E. Thyrhaug, S. Petersen, J.A. Meyer, N. Bovet, T. Vosch, J. Nygård, X. Qiu, W. Hu, Y. Liu, G.C. Solomon, H.G. Kjaergaard, T. Bjørnholm, M.B. Nielsen, B.W. Laursen, K. Nørgaard, Ultrathin reduced graphene oxide films as transparent top-contacts for light switchable solid-state molecular junctions, Adv. Mater. 25 (2013) 4164–4170.
[89] G.G.D. Han, H. Li, J.C. Grossman, Optically-controlled long-term storage and release of thermal energy in phase-change materials, Nat. Commun. 8 (2017) 1446.
[90] A.A. Beharry, O. Sadovski, G.A. Woolley, Azobenzene photoswitching without ultraviolet light, J. Am. Chem. Soc. 133 (2011) 19684–19687.
[91] D. Bléger, J. Schwarz, A.M. Brouwer, S. Hecht, *o*-Fluoroazobenzenes as readily synthesized photoswitches offering nearly quantitative two-way isomerization with visible light, J. Am. Chem. Soc. 134 (2012) 20597–20600.
[92] D.B. Konrad, J.A. Frank, D. Trauner, Synthesis of redshifted azobenzene photoswitches by late-stage functionalization, Chem. Eur J. 22 (2016) 4364–4368.
[93] S. Samanta, C. Qin, A.J. Lough, G.A. Woolley, Bidirectional photocontrol of peptide conformation with a bridged azobenzene derivative, Angew. Chem. Int. Ed. 51 (2012) 6452–6455.
[94] S. Crespi, N.A. Simeth, B. König, Heteroaryl azo dyes as molecular photoswitches, Nat. Rev. Chem. 3 (2019) 133–146.
[95] S. Crespi, N.A. Simeth, A. Bellisario, M. Fagnoni, B. König, Unraveling the thermal isomerization mechanisms of heteroaryl azoswitches: phenylazoindoles as case study, J. Phys. Chem. A 123 (2019) 1814–1823.
[96] J. Calbo, C.E. Weston, A.J.P. White, H.S. Rzepa, J. Contreras-García, M.J. Fuchter, Tuning azoheteroarene photoswitch performance through heteroaryl design, J. Am. Chem. Soc. 139 (2017) 1261–1274.
[97] C.E. Weston, R.D. Richardson, P.R. Haycock, A.J.P. White, M.J. Fuchter, Arylazopyrazoles: azoheteroarene photoswitches offering quantitative isomerization and long thermal half-lives, J. Am. Chem. Soc. 136 (2014) 11878–11881.
[98] C.E. Weston, R.D. Richardson, M.J. Fuchter, Photoswitchable basicity through the use of azoheteroarenes, Chem. Commun. 52 (2016) 4521–4524.
[99] C.E. Weston, A. Krämer, F. Colin, Ö. Yildiz, M.G.J. Baud, F.J. Meyer-Almes, M.J. Fuchter, Toward photopharmacological antimicrobial chemotherapy using photoswitchable amidohydrolase inhibitors, ACS Infect. Dis. 3 (2017) 152–161.